CHALMERS
UNIVERSITY OF TECHNOLOGY

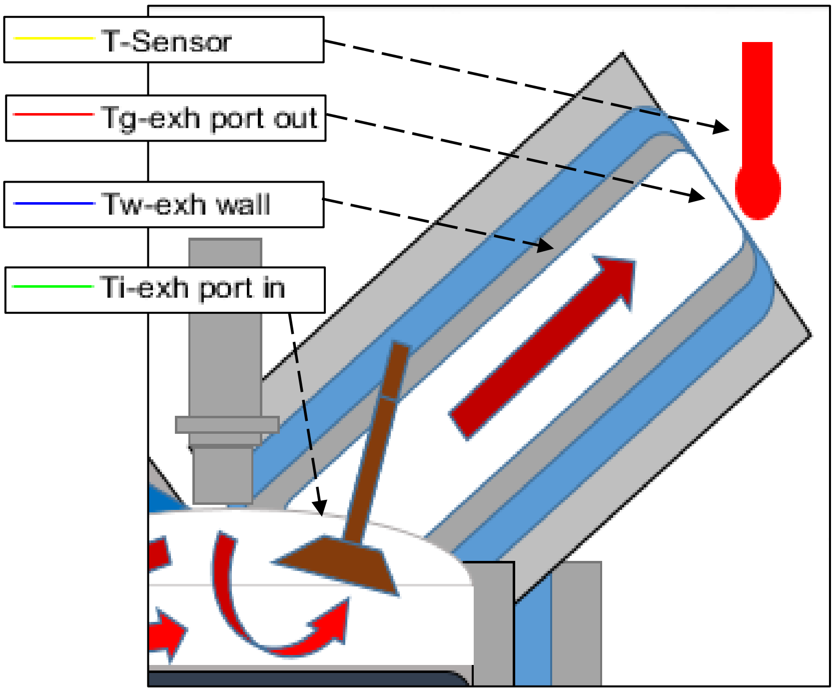

DIESEL ENGINE OUT EXHAUST TEMPERATURE MODELLING

Moving from a map based to physically based model approach

Master's thesis in Automotive Engineering

SUDIP SARKAR

JAYESH GHARTE

Department of Applied Mechanics
CHALMERS UNIVERSITY OF TECHNOLOGY
Gothenburg, Sweden 2017

MASTER THESIS 2017 Number: 89

DIESEL ENGINE OUT EXHAUST TEMPERATURE MODELLING

Moving from a map based to physically based model approach

Sudip Sarkar

Jayesh Gharte

Department of Applied Mechanics, Division of Combustion
CHALMERS UNIVERSITY OF TECHNOLOGY
Goteborg, Sweden 2017

Diesel Engine Out Exhaust Temperature Modelling
Moving from a map based to physically based model approach
SUDIP SARKAR
JAYESH GHARTE

Supervisor: - Anders Boteus, Martin Larsson
Examiner: - Sven B. Andersson

Master Thesis 2017: 89
ISSN: 1652-8557

Department of Applied Mechanics
Division of Combustion
Chalmers University of Technology
SE-412 96 Göteborg
Sweden
Telephone: + 46 (0)31-772 1000

Cover: Illustration of gas flow through exhaust port, Section 2.3.1 Figure 5

Department of Applied Mechanics
Göteborg, Sweden 2017

DIESEL ENGINE OUT EXHAUST TEMPERATURE MODELLING
Moving from a map based to physically based model approach

Master thesis in Automotive Engineering
SUDIP SARKAR
JAYESH GHARTE

Department of Applied Mechanics
Division of Combustion
Chalmers University of Technology

ABSTRACT

Engine out exhaust gas is an input to the engine system components downstream, which are directly or indirectly responsible for air charge control, emission regulation, torque control or are used as feedback to the engine control system. This makes the accurate prediction of the exhaust gas an important criterion for the control system. Automotive manufacturers use map based models for the prediction of exhaust temperature at known engine operating conditions. The aim of this thesis is to design a predictive physically based exhaust temperature model for a typical diesel engine. The model predicts the temperature of the exhaust gases at the end of the exhaust port with acceptable levels of accuracy. Previously available map based models were specific to the engine and required extensive test data for creation and validation of such maps. The model developed in this thesis is physically based, which enables its usage across a range of typical diesel engines with reasonable modifications. This thesis also includes two different modelling approaches for the temperature prediction. One being an averaged out cyclic approach while the other being a more resolved computation at crank angle degrees. Data from test rig is used as input parameter for calibrating and tuning the models. An attempt to understand the transient effects at the end of the exhaust port is also a part of the thesis and precedes the discussion on modelling.

Keywords: - Diesel Engine, Engine Out Exhaust Temperature, Heat Transfer, Hohenberg Overall Heat Transfer, Crank Angle Resolved Model, Dual Cycle Model, Wiebe's Curve, Mass Fraction Burnt, Calibration, Tuning, Optimization, Transient Behaviour, Temperature Sensor, Part Load Test

ACKNOWLEDGEMENT

We would like to thank Volvo Cars and Chalmers for creating this exciting opportunity to work on such an interesting problem statement. We would like to thank our supervisor Martin Larsson for the valuable guidance, feedback, technical inputs and much required course corrections along the way. Our innumerable queries could neither reach the limit of his patience nor did our occasional persistence deter him from encouraging us to explore wider horizons. We would like to thank our manager Anders Boteus for facilitating us and creating the perfect work environment. The support we received from him prompts us to set new benchmarks in our perception of an ideal manager. We also would like to thank all those in the department and outside who were glad to give us their valuable time and share their knowledge and experiences. Finally, we would like to thank our examiner at Chalmers, Professor Sven B. Andersson for helping us lay the necessary academic foundation on which all of the work is based. We find ourselves to be very fortunate being encouraged by him to explore, persevere, strive for continuous improvements till we succeed.

Nomenclature

Symbol	Description	Unit
x_b	Fuel mass fraction burned	-
M_1	The efficiency parameter of the Wiebe function	-
M_2	The form factor of the Wiebe function	-
θ_{dur}	Combustion duration	Degree
θ	Crank angle	Degree
θ_b	Crank angle at start of combustion	Degree
T_1	Intake air charge temperature	K
m_{egr}	Mass flow rate of EGR gasses	Kg/s
w_{air}	Mass flow rate of the fresh air charge	Kg/s
$T_{em_{prev}}$	Temperature in the exhaust manifold at the end of previous cycle	K
T_{in}	Intake air temperature	K
γ_1	Ratio of the specific heat	-
C_{p_1}	Specific heat at constant pressure	$KJ/Kg\ K$
C_{v_1}	Specific heat at constant volume	$KJ/Kg\ K$
P_2	Pressure inside the cylinder when piston is at TDC	N/m^2
P_1	Pressure inside the cylinder when piston is at BDC	N/m^2
V_1	Volume occupied by gas when piston is at BDC	m^3
V_2	Volume occupied by gas when piston is at TDC	m^3
T_2	Temperature inside the cylinder after compression stroke	K
T_{w1}	Assumed wall temperature which is equivalent to the T1	K
m_1	Mass flow rate of both EGR gasses and fresh air	Kg/s
h_g	Overall heat transfer coefficient for exhaust gas	W/m^2K
$C1$	Hohenberg coefficient 1	-
$C2$	Hohenberg coefficient 2	-
sp	Piston velocity	m/s
$T_{2_{ht}}$	Temperature after heat transfer	K
C_v	Specific heat at constant volume	$KJ/Kg\ K$
h_c	Convective heat transfer coefficient of coolant	W/m^2K
A_g	Area available to gases in cylinder for heat transfer	m^2
T_{w2}	Wall temperature after heat transfer	K
A_c	Area available to coolant around cylinder for heat transfer	m^2
T_{3a}	Temperature at the end of constant volume combustion	K
w_{fuel}	Mass of fuel injected	Kg
x_{cv}	Mass fraction of fuel burnt at constant volume	-
q_{hv}	Calorific value of Diesel fuel	J/Kg

P_{3a}	Pressure at the end of constant volume combustion	N/m^2
P_2	Pressure at the end of Compression	N/m^2
V_{3a}	Volume at the end of constant volume combustion	m^3
m_2	Total mass available for heat transfer after constant volume combustion	Kg
$T_{3a_{ht}}$	Temp. at the end of constant volume combustion after heat transfer	K
$T_{w_{3a}}$	Temp. of cylinder walls after constant volume combustion	K
T_3	Temperature at the end of constant volume combustion	K
V_3	Volume at the end of constant volume combustion	m^3
m_{3_a}	Total mass available for heat transfer after constant pressure combustion	Kg
C_{v3a}	Specific heat at constant volume	$KJ/Kg\ K$
$T_{3_{ht}}$	Temp. at the end of constant pressure combustion after heat transfer	K
T_{w3}	Temp. of cylinder walls after constant pressure combustion	N/m^2
P_4	Pressure at the end of expansion	N/m^2
V_4	Volume at the end of expansion	m^3
T_4	Temperature at the end of expansion	K
m_3	Total mass available for heat transfer during expansion	Kg
$T_{4_{ht}}$	Temp. at the end of expansion after heat transfer	K
$T_{w_{port}}$	Exhaust port wall temperature	K
$h_{g_{port}}$	Gas heat transfer coefficient in port	W/m^2K
A_{gw}	Area available for heat transfer from gas to port wall	m^2
A_{cw}	Area available for heat transfer from coolant to port wall	m^2
m_{port}	Mass in the control volume of port	Kg
$\mathrm{T1}_{\mathrm{ht(n)}}$	Temperature after heat transfer at n where n is the crank angle degree	K
T_{im}	Temperature of air in intake manifold	K
$P_{1_{(n)}}$	Pressure at intake at n where n is the crank angle degree	N/m^2
$\gamma_{(n)}$	Gamma at CAD n	-
$C_{p(n)}$	Specific heat at constant pressure at CAD n	$KJ/Kg\ K$
$C_{v(n)}$	Specific heat at constant volume at CAD n	$KJ/Kg\ K$
$T_{w1_{(n)}}$	Wall temperature at CAD n	K
$theta_{(n)}$	Crank Angle Degree	Degree
$fuel_{br_{(n)}}$	Mass of fuel burnt at CAD n	Kg
$h_{g_{cmb(n)}}$	Overall heat transfer coefficient for crank angle n	W/m^2K
$T_{modelled}$	Modelled Exhaust gas Temperature at the end of Exhaust port	K
$T_{measured}$	Measured Exhaust gas Temperature at the end of Exhaust port	K

Abbreviations

BDC	Bottom Dead Center
CAD	Crank Angle Degrees
CAE	Computer Aided Engineering
DPF	Diesel Particulate Filter
EGR	Exhaust Gas Recycling
HT	Heat Transfer
IAT	Intake Air Temperature
MAF	Mass Air Flow
PV	Pressure vs Volume
TDC	Top Dead Center
Y	Y axis of the plot
X	X axis of the plot

Contents

1. Introduction

This thesis is conducted in cooperation with Volvo cars and Chalmers University of Technology. Aim of the thesis is to design a physically based exhaust temperature model to predict the engine out exhaust gas temperature at end of the exhaust port of a typical diesel engine. The modelling of the exhaust temperature is useful for turbo protection and as a control signal for systems downstream of the exhaust ports.

1.1 Background

Increasing volumes of vehicle units sold every year has led to a surge of emission levels in the environment. In order to control the levels of emission, legislations are getting stringent. These governing policies have put the automakers in a dilemma to come up with better solutions to meet these regulations while keeping the price and performance reasonable. Car manufacturers have been travailing to design many complex systems to overcome this legislation problem without compromising the performance and fuel economy of the vehicle. An understanding of the engine out exhaust temperature levels leads to a better predictability and control of the system. To measure the temperature at end of exhaust becomes a very critical task but with the absence of a sensor at this location in a stock vehicle, the temperature has to be modelled. Two approaches that can be used to design such a complex system can be a map based or an equation based predictive model.

Currently, map based modelling approach is being used by the automakers to predict final exhaust temperature at the end of the port, unfortunately, this approach may have limitations that need to be solved by using new approaches. The map based model is based on extensive testing and calibration of the maps. This can be a unique process for each engine thereby deviating from a general solution of the problem. The maps used can be seen as black boxes which cannot be correlated to physical phenomenon of the processes in the cylinder. Development of physically based model can eliminate these riddles that occurs in map based model.

1.2 Thesis Goal

The main goal of this master thesis is to develop a model that can be used to predict the engine out exhaust gas temperature of the diesel engine. The developed model should be physical or equation based, easy to understand and have acceptable level of accuracy. The model can be optimized and implemented in the existing control system.

2. Physical System

This section describes the physics based approach to model the processes occurring in cylinder and port. Some important aspects relevant to the entire 4 stroke cycle and the transience effects are discussed in following subsections. Three locations of interest for modelling purposes are, combustion chamber, exhaust port and the sensor itself.

2.1 Combustion Chamber

Steady state operation of the engine is a rare occurrence in the actual drive cycle. Yet the knowledge of engine performance and characteristics at steady state operating points allows much better understanding of the system functionality. This can further be developed into a physical model which can accommodate for different time dependencies. The combustion chamber is the location where chemical energy of fuel converts into other forms of energy. The mechanical output is only a fraction of this energy. While the rest is dispersed as heat losses, noise, losses through the exhaust gases and other phenomenon. The processes occurring in the combustion chamber within a cycle can be broadly studied in four stages as discussed in following subsections.

2.1.1 Intake

The intake air charge flows in through the air filter into the turbocharger where it is compressed and sent to the charge air cooler. The pressurized air charge is collected in the intake manifold and then distributes into the intake ports. The exhaust gases are recirculated and mixed with the fresh air charge in the intake manifold. The manifold design allows the intake air charge to acquire the desired amount of swirl to facilitate better mixing and combustion. The swirl is controlled by a control signal operating a valve in the manifold. The MAF sensor signal provides the air flow through the manifold. The IAT sensor detects the temperature of the intake air. The pressure sensor at the output of the turbocharger measures the boost pressure. The pressure of air after charge air cooler is either modelled or measured with a sensor. The important valve event for this process are the intake valve opening and closing. The Intake valve opens a few crank angle degrees after TDC and closes a few crank angle degrees after BDC. The late intake valve opening is typically to avoid any valve overlap situation.

2.1.2 Compression

The air charge that enters the cylinder starts getting compressed as soon as the piston starts moving from BDC towards TDC. The compression process in an ideal dual cycle is assumed to be isentropic/ adiabatic where no heat or mass is lost from the system to the surroundings. The system being the closed cylinder with air charge trapped inside it. In this process work is done by the piston on the gases to compress it. The adiabatic correlation leads us to a specific value of gamma, which is the ratio of the specific heat capacity at constant pressure and specific heat capacity at constant volume. The compression of the gases continue till the piston reaches the TDC. The heat capacities are a function of the temperature of the gas in the system. The temperature of the gases gradually increases as the volume decreases and this leads to a final temperature at the end of the process. This implies that we have a different gamma for each operating point of the engine.

2.1.3 Combustion

The process of combustion is a heat release process that occurs due to conversion of chemical energy of the fuel to thermal energy. Some important phenomenon related to combustion are discussed in the following subsections.

2.1.3.1 Injection Timing

The injection of the fuel occurs at a predetermined CAD. This is specific to the control system of the engine. The injection of fuel is done in pulses. The pulses may consist of a main pulse, pilot injection pulses and post injection pulses. The Major fraction of the fuel meant to produce torque is injected in the main injection. The post injection is meant to prolong the combustion process. This late injection can be used to increase the temperature of the exhaust gases by allowing some fuel to burn downstream of the exhaust manifold. This may help in the oxidation of soot in the DPF of the exhaust aftertreatment system. In the system that we model, the energy released from the fuel is assumed to be only from the main injection.

2.1.3.2 Rate of Heat release

The heat release in case of an averaged heat release rate computation can be directly obtained by calculating the total chemical energy content in the total mass of fuel burned. This simplification overlooks the time or CAD dependency of the heat release rate. Alternately, the rate of heat release in diesel engines can be computed for each CAD from the thermodynamic laws [1].

$$\frac{dQ_n}{dt} = \frac{\gamma}{\gamma - 1}\, p\, \frac{dV}{dt} + \frac{1}{\gamma - 1}\, V\, \frac{dp}{dt} \qquad (1.)$$

This formulation requires the pressure trace within the cylinder. A control system in the vehicle does not make this measurement and therefore a different approach has to be taken to compute the heat release rate. This system uses a Wiebe's correlation to develop a heat release rate profile *(Figure 1)*.

$$x_b = \left(1.0 - exp\left(-M_1 * \left(\frac{\theta - \theta_b}{\theta_{dur}}\right)^{M_2+1}\right)\right) \qquad (2.)$$

Wiebe's correlation defines the mass fraction of fuel burned for a given crank angle degree. The mass fraction burned is a function of the combustion duration and start of combustion crank angle degree. The coefficients M1 & M2 are optimized for the model to generate a desired exponential curve.

2.1.3.3 Constant Volume and Constant Pressure

The combustion in an ideal Otto cycle is at constant volume and combustion in an ideal Diesel cycle occurs at constant pressure. Based on previous studies, a combined approach has been found to be more accurately depicting a real engine cycle [1]. In case of the Dual cycle approach, we assume combustion to begin at constant volume and then transition into constant pressure combustion. The illustration represents different parts of the cycle in the Pressure versus Volume plot *(Figure 2)*.

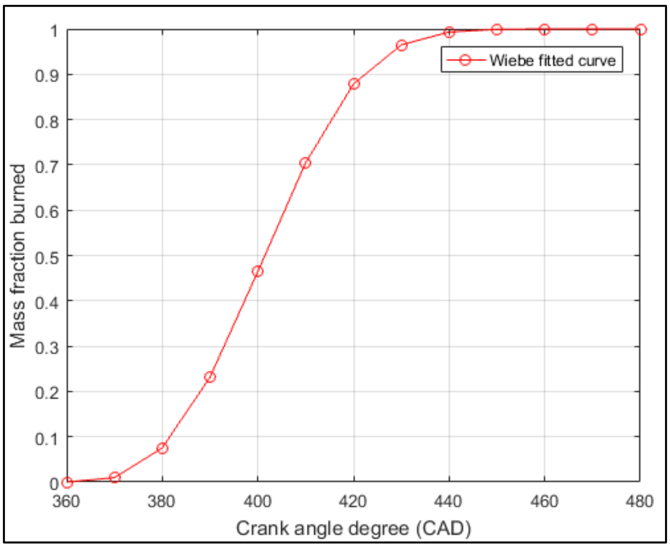

Figure 1: - Typical Wiebe's Curve. Y-Fuel Mass Fraction burnt, X-CAD.

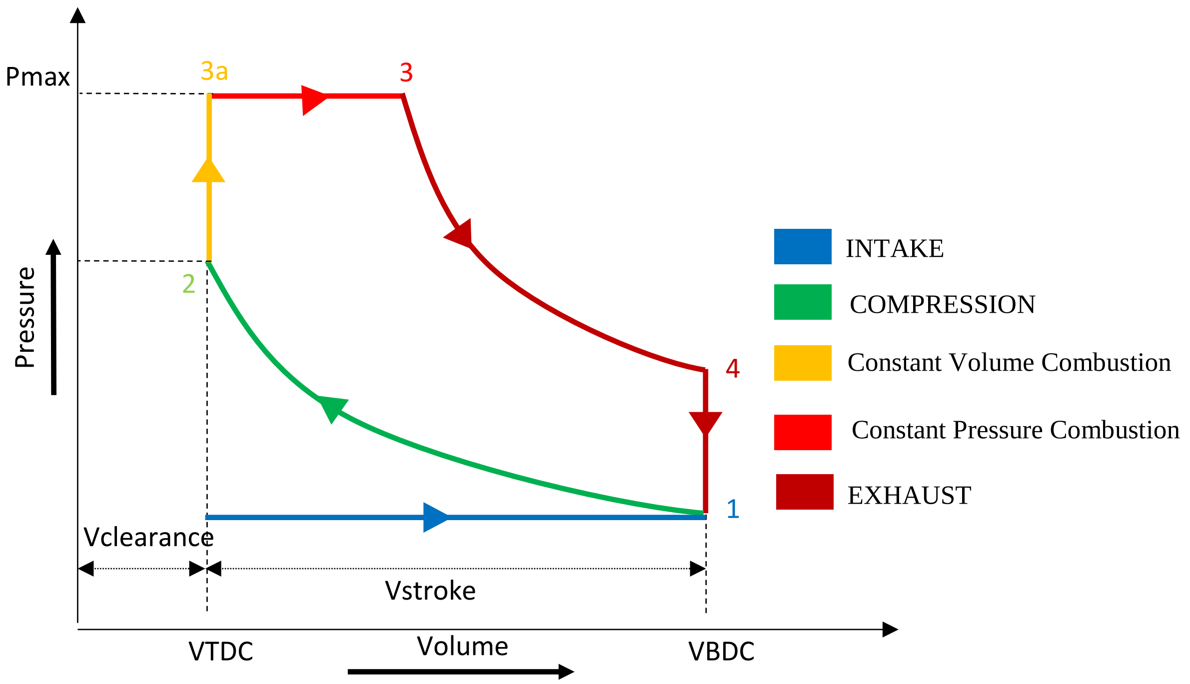

Figure 2:- Ideal Dual Cycle P-V Diagram

2.1.4 Expansion

During this stage of the cycle, the combustion gases in the cylinder expand in volume as the piston moves from the TDC to BDC. This expansion can be considered identical to an adiabatic expansion. Since the system is similar to a closed system, there is no mass or heat transfer into or out of it. Work is done by the piston on the gases to expand them. The adiabatic expansion is assumed to have a certain gamma value. This is determined by the specific heat con at constant volume and constant pressure.

2.2 Exhaust Port

The port can be geometrically approximated as a hollow metallic tube with a certain wall thickness. The flow of the gases through the port and the loss of heat out of the control volume of the port determine the final port out temperature levels. The pulsation effects in the port are also discussed in the section.

2.2.1 Exhaust

The last phase of the cycle includes expulsion of the exhaust gases out of the cylinder. The gases move out through the exhaust valve as it opens. The system pressure equals the pressure at the exhaust port at this stage.

2.2.2 Heat Transfer

Heat Transfer is one of the significant sources of energy loss from the system [1]. Heat is lost in all the stages of the cycle and through several components of the engine. Cylinder walls, cylinder head, piston, exhaust port are the primary locations from where heat is lost from the system. The coolant present around the cylinder walls carries away this lost heat from the system to the radiator, from where it is dissipated into the atmosphere.

2.2.3 Port flow pulsation

The exhaust gas flow through the control volume in the exhaust port is a time varying quantity. This can be visualized by a plot of mass flow of gas through port with respect to crank angle degrees. The CAE data of a simulated engine has been depicted in the figure below *(Figure 3)*. There is no mass flow when the exhaust valve is closed, but on opening two pulses can be observed with different peak values. The Exhaust temperature profile however has three peaks during the exhaust valve closed duration, followed by a larger peak when the exhaust valve opens. The additional peaks in temperature are the pulsation effects from the exhaust manifold.

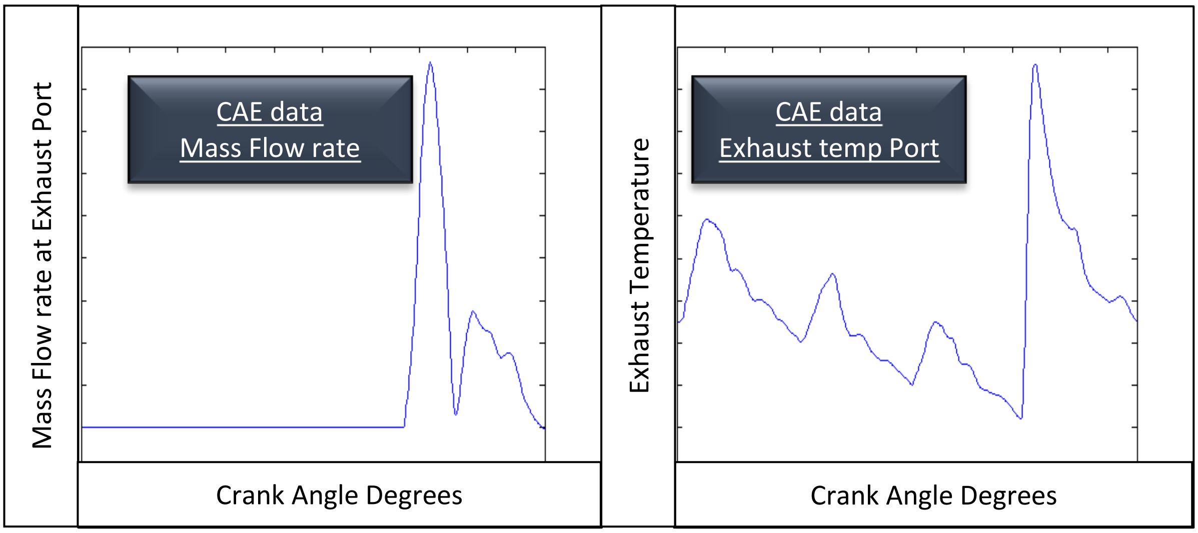

Figure 3:- Plots from CAE data. Y (left) -Simulated Mass flow rate & Y (right) - Simulated Exhaust temperature, X-CAD

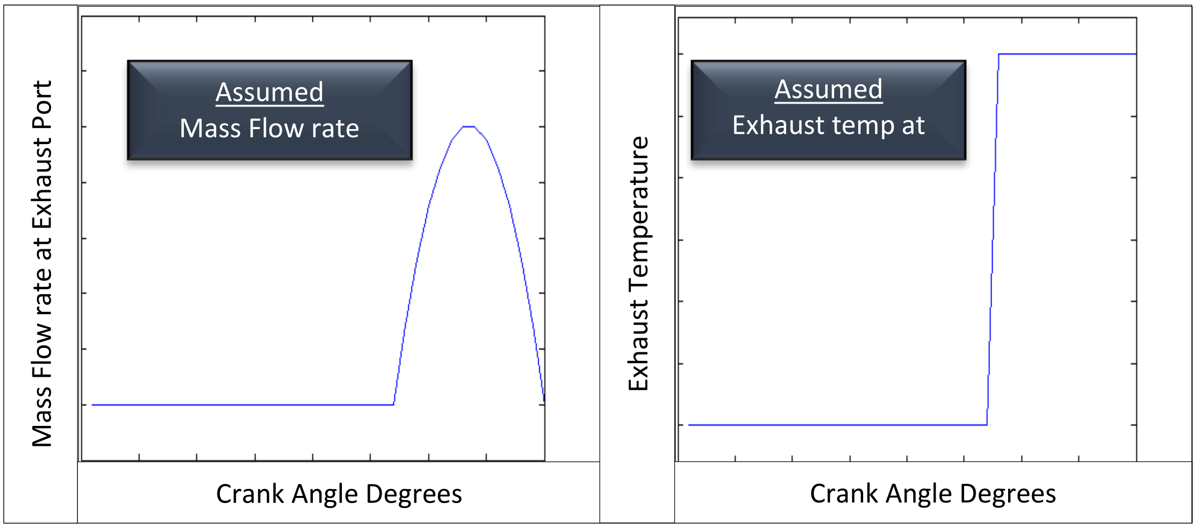

Figure 4:- Waveforms assumed for the transient model. Y (left) -Mass flow rate & Y (right) - Exhaust temperature, X-CAD.

The CAE data is used as a reference to develop an input signal for the transient model. A quadratic cam profile is assumed and a mass flow pulse is developed based on it. The exhaust temperature along crank angles can be assumed to have two steady levels of temperature, one, when the valve is closed and the other when it is open. This is represented in the pulse as shown below *(Figure 4)*.

2.3 Temperature Sensor

The system has certain types of transience which are studied and the effects are understood. The transient model developed for this purpose is a separate model, simulating the transient equations in the system. The parameters though in the model are not tuned as the purpose of the model is to only study the transient behavior and not to accurately quantify it. However, the temperature sensor characteristics used for the model are according to the specifications provided by the supplier of sensors at engine test rigs.

2.3.1 Transient Sensor measurements

The pulses assumed for the mass flow and the exhaust temperature are used as input for the transient model in Simulink. This enables a study of the temperature profiles at different locations in the system. The illustration *(Figure 5)* represents the locations at which the time varying temperature profiles are computed in the model.

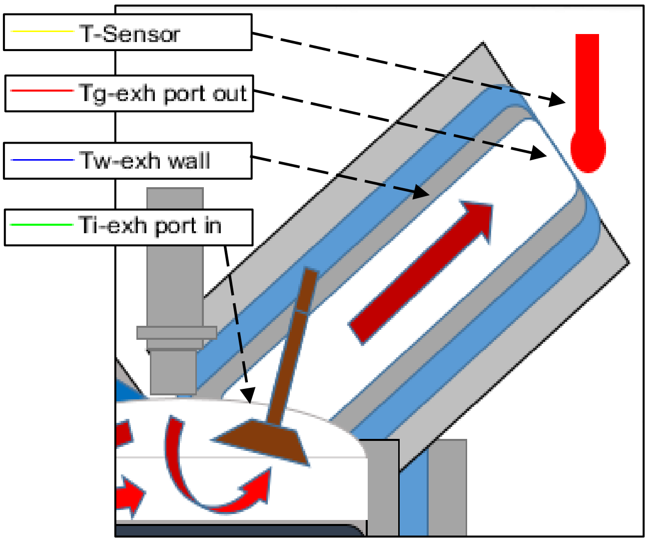

Figure 5:- Illustration of gas flow through exhaust port. Signal colours depicted as used in the transient model plots

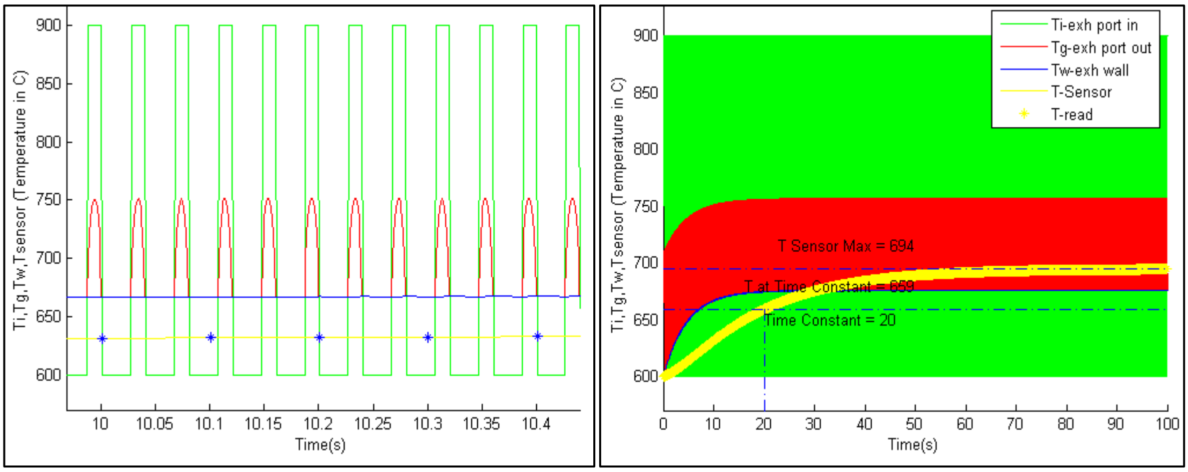

Figure 6 :- Transient Model temperature output at various locations. Left- Temperature Pulses viewed within a scale of 0.5 second. Right – Temperature Profiles viewed over a period of 100 seconds.

The output pulses from the transient model are as shown in the plot below *(Figure 6)*. The color of the pulses indicates the location at which they are modelled. The transience can be observed for the pulses. The time frame on the axis is very short i.e. about 10 seconds. This is not sufficient to visualize the transient growth of the temperature signal. For this purpose, a longer time duration of about 100 seconds is observed. The closely spaced green pulse give an impression of a green band as do the other colored signals. This plot however enables us to see the transient growth of the signal with respect to time. The final measured exhaust temperature reaches a final steady state value after a delay of several seconds with a time constant of around 20 seconds in this case.

2.3.2 Parameter variation effect on transient and steady state

Transient response study is necessary to understand the behaviour of the model under different varied input parameters. Basically, in transient response, many input characteristics of model such as material density, engine load and other heat transfer coefficient for coolant & Gas have been changed to see the effect on the model's transient behaviour. The evaluated values for temperatures can be analysed for two characteristics i.e. time constant of the signal (transient behaviour) and the final steady state value. The plots in successive subsections represent the transient behaviour on the left y-axis (in red) and the steady state value on the right y-axis (in black). The variation of these parameters allows us to understand their effects on the steady or transient characteristics.

2.3.2.1 Sensor probe diameter

In following *(Figure 7)*, effect of variation of sensor probe diameter is seen on the model output parameters. As the diameter increases, the time constant also increases gradually due to change in surface area of the sensor to sense

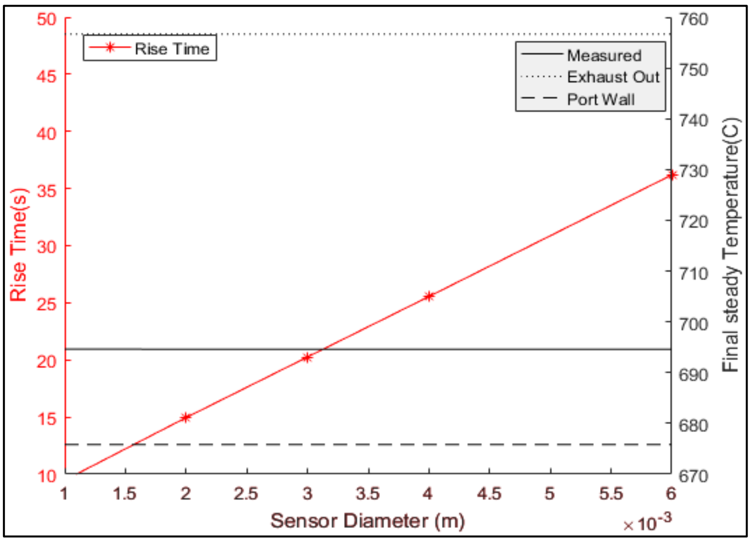

Figure 7 :- Effect of variation of sensor diameter on time constant and Final steady state Temperatures. Y (left) - Transient characteristic of time constant of the exhaust gas temperature at end of exhaust port. Y (right) – Final steady state Temperatures, X- Sensor diameter.

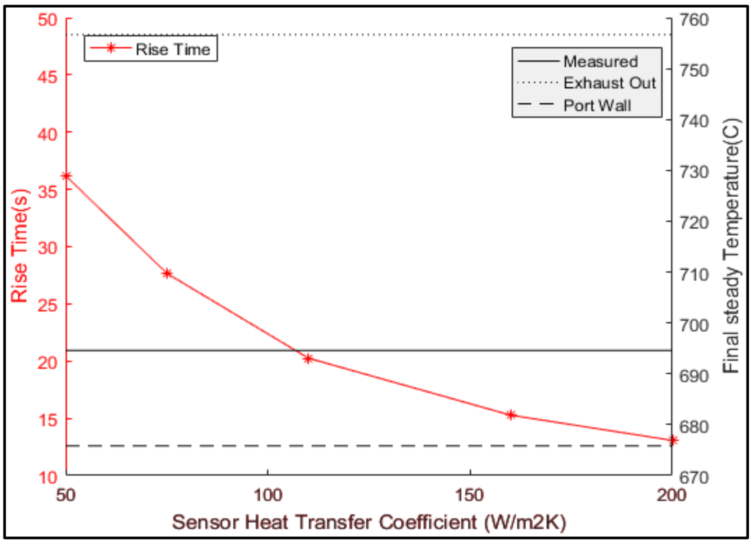

Figure 8 :- Effect of variation of sensor heat transfer coefficient on time constant and Final steady state Temperatures. Y (left) - Transient characteristic of time constant of the exhaust gas temperature at end of exhaust port. Y (right) – Final steady state Temperatures, X- Sensor heat transfer coefficient.

the gas temperature, but rest of the parameters such as Exhaust temperature, port wall temperature, and measured value remain constant for each varied sensor diameter. In this plot sensor diameter has been varied from 3 mm to 6 mm at 5 different intervals.

2.3.2.2 Sensor heat transfer coefficient

Heat transfer coefficient is also one of the main factors that need to be considered for understanding the transient effect. As shown in following *(Figure 8)*, time constant decreased when heat transfer coefficient of the sensor material increased for each given interval. Heat transfer coefficient value varied from 50 (W/m2K) to 200 (W/m2K) at 5 different intervals.

2.3.2.3 Port material

Density of the material also influences heat transfer phenomenon. In *(Figure 9)*, effect of varied port material density can be seen. With varied density of port material, time constant of sensor also increased gradually, but there is no effect on the final steady state levels.

2.3.2.4 Coolant temperature

In the following *(Figure 10)* we see that transient response of coolant temperature does not show any significant influence on the model output parameters and time constant, but even then very minor rise can be seen for the final steady state temperature whereas there is no effect on the transient nature of the signal.

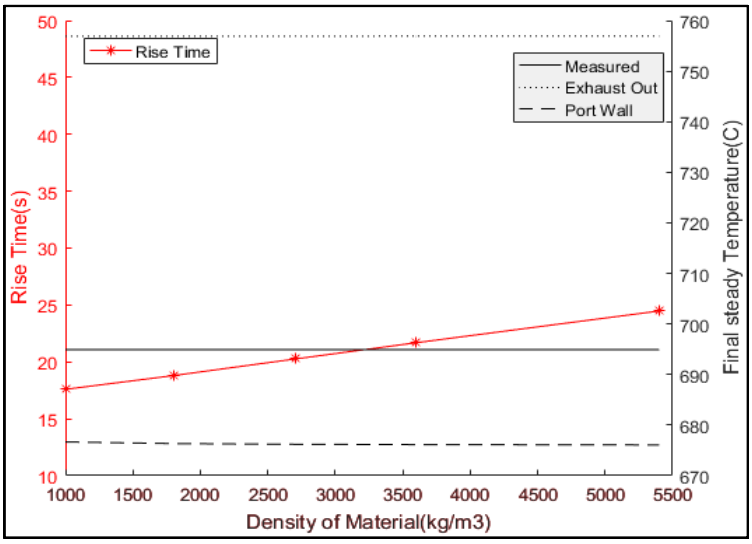

Figure 9 :- Effect of variation of port wall material density on time constant and Final steady state Temperatures. Y (left) - Transient characteristic of time constant of the exhaust gas temperature at end of exhaust port. Y (right) – Final steady state Temperatures, X- Port wall material density.

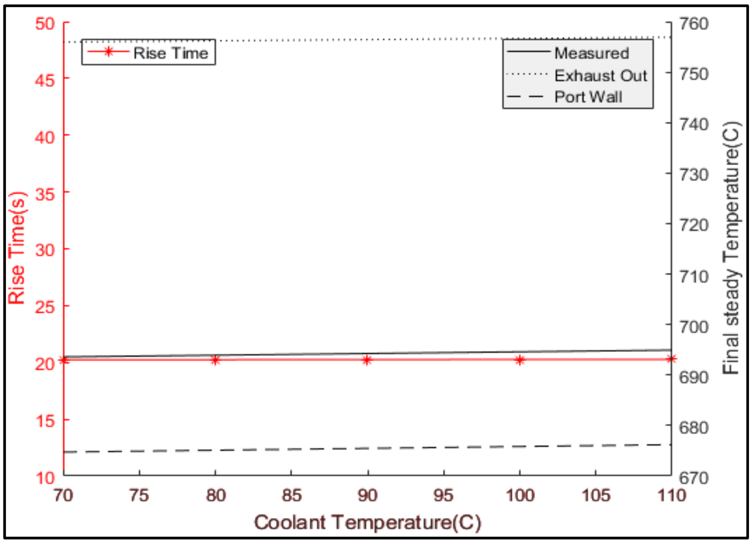

Figure 10 :- Effect of variation of Coolant Temperature on time constant and Final steady state Temperatures. Y (left) - Transient characteristic of time constant of the exhaust gas temperature at end of exhaust port. Y (right) – Final steady state Temperatures, X- Coolant Temperature.

2.3.2.5 Average temperature

The band input signal representing the exhaust temperature at the valve increases with the load on the engine. An increase in the average band temperature is indicative of increase in load. There is no change in time constant with change in load. The steady levels of the temperature profiles however increase linearly with the engine load. In this case the average band temperature is varied from 400C to 800C to simulate different load conditions. It is illustrated in *(Figure 11)*.

2.3.2.6 Convective heat transfer coefficient of the coolant.

Following *(Figure 12)* shows the effect of the convective heat transfer coefficient of coolant on model output parameters when it varies consecutively from lower value 50 (W/m2K) to 200 (W/m2K) for five different intervals in between. It is observed that the increasing value of convective heat transfer coefficient of coolant in the model has no effect on the time constant but the steady temperature levels gradually decrease.

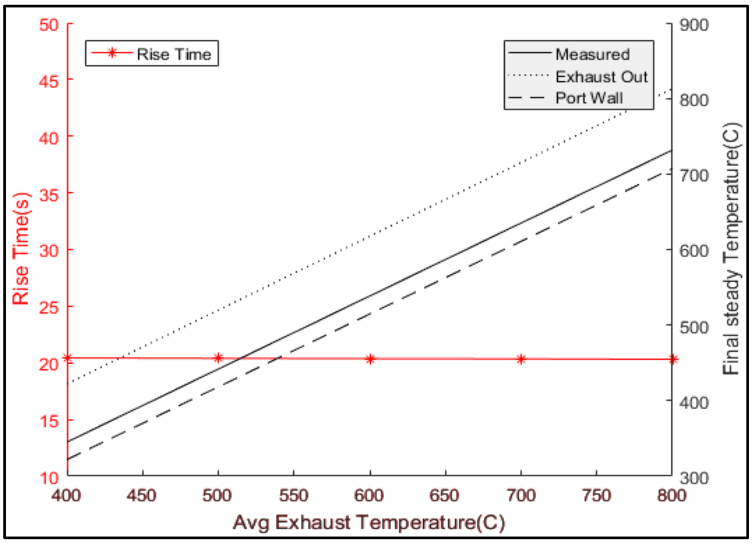

Figure 11 :- Effect of variation of Average cylinder out exhaust temperature on time constant and Final steady state Temperatures. Y (left) - Transient characteristic of time constant of the exhaust gas temperature at end of exhaust port. Y (right) – Final steady state Temperatures, X- Average cylinder out exhaust temperature.

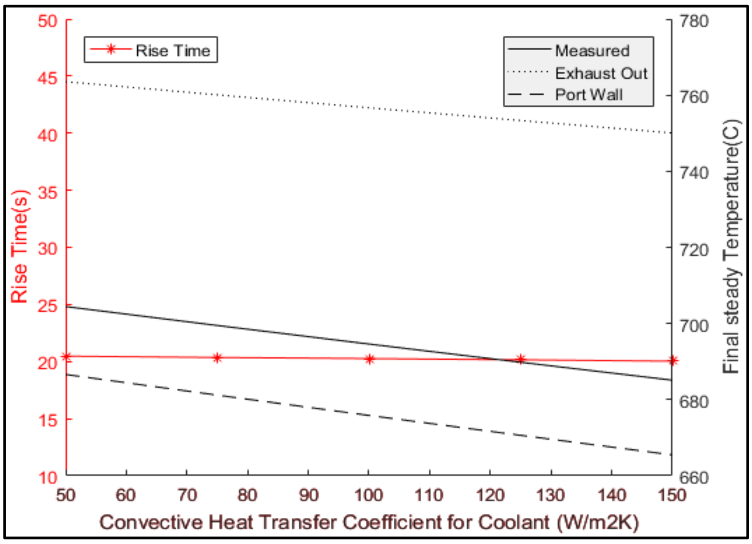

Figure 12 :- Effect of variation of coolant convective HT coefficient on time constant and Final steady state Temperatures. Y (left) - Transient characteristic of time constant of the exhaust gas temperature at end of exhaust port. Y (right) – Final steady state Temperatures, X- Coolant convective HT coefficient.

2.3.2.7 Heat transfer coefficient of the gas.

In following *(Figure 13)*, we see the effects of varying the overall heat transfer coefficient of the gas. As the overall heat transfer coefficient of gas increases from 1000 (W/m2K) to 5000 (W/m2K), the time constant decreases. The temperature measured at sensor and the port wall temperature both increase. But we can see a decrease in the exhaust gas temperature out of the exhaust port.

2.3.2.8 Engine speed

In the following *(Figure 14)*, the engine speed parameter has changed the time constant trend slightly and it means that time constant is a directly dependant variable of the engine speed. Engine speed mainly influences the exhaust out temperature whereas port wall temperature and the measured gas temperature at the sensor remain almost constant.

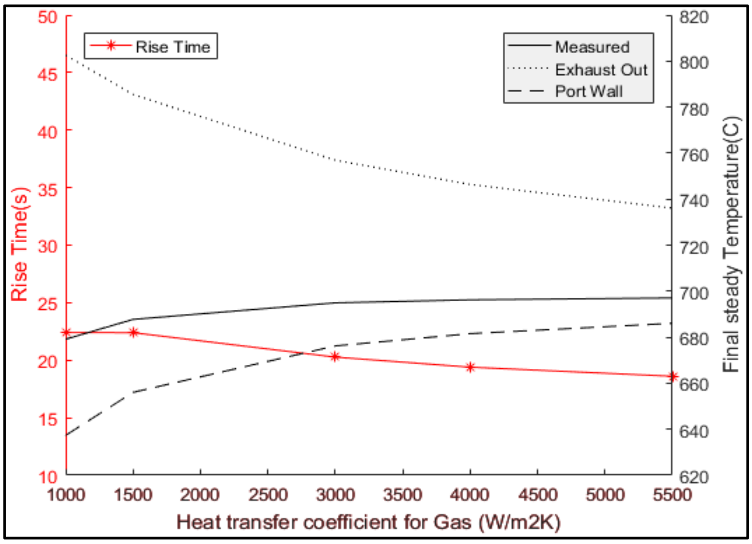

Figure 13 :- Effect of variation of gas overall HT coefficient on time constant and Final steady state Temperatures. Y (left) - Transient characteristic of time constant of the exhaust gas temperature at end of exhaust port. Y (right) – Final steady state Temperatures, X- Gas overall HT coefficient.

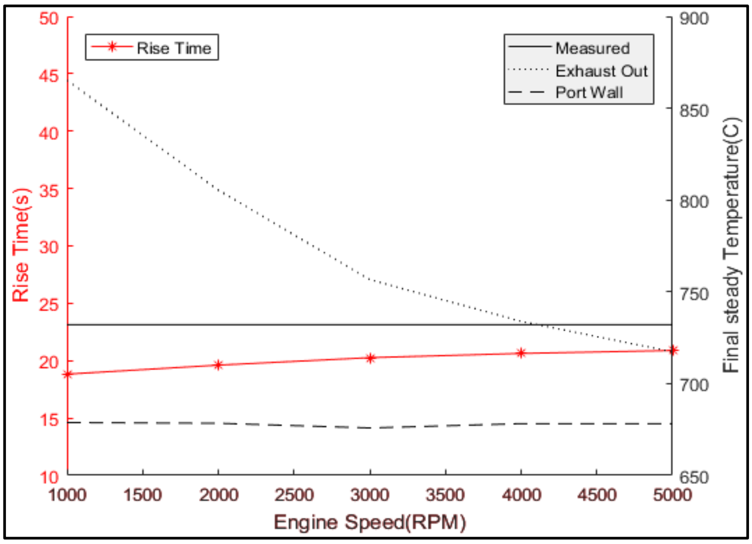

Figure 14 :- Effect of variation of Engine speed on time constant and Final steady state Temperatures. Y (left) - Transient characteristic of time constant of the exhaust gas temperature at end of exhaust port. Y (right) – Final steady state Temperatures, X-Engine Speed.

3. Modelling

There are two different modelling approaches explored in this section. The first approach is a generalized one and intends to be simple and less computationally demanding for the control system. The second model aims at capturing more detailed attributes of each cycle and is resolved in crank angle degrees.

3.1 Dual Cycle Model

This model is based on a combination of the Otto cycle and the diesel cycle wherein the combustion part of the cycle partially takes part at constant pressure and partially at constant volume. All the steps of the Cycle are described below *(Figure 15)* with the physical equations governing them.

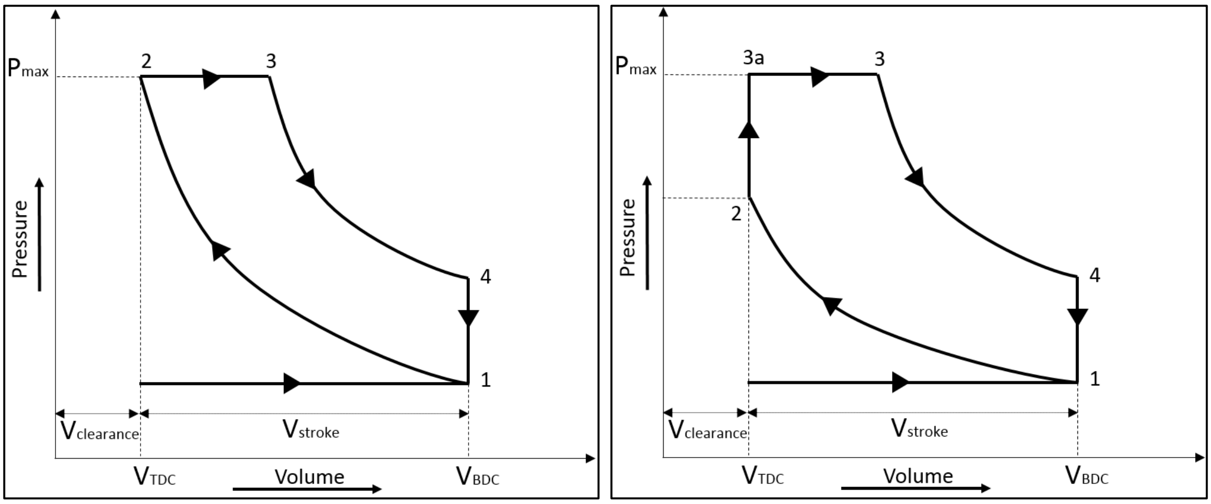

Figure 15 :- Pressure-Volume Diagram. Left- Typical P-V diagram for diesel cycle. Right- Typical P-V Diagram for dual cycle.

The intake air charge characteristics at the end of the intake stroke are measured parameters. The charge air temperature and pressure are the parameters recorded after the charge air cooler. The initial volume at the beginning of compression stroke i.e. when the piston is at TDC, is the clearance volume.

3.1.1 Intake stroke

The fresh air charge is sucked in through the air filter and then finally reaches the intake manifold. The fresh charge is mixed with exhaust gases that are recirculated into the intake to reduce the flame temperatures. The signal from the mass air flow sensor is used to calculate the air mass flow rate. The intake air temperature sensor gives the temperature of the incoming charge. The effective temperature of the charge after the Charge air cooler is acquired from an existing model in the control system. The final temperature of the air charge is the balance between the temperature of the fresh air charge and the EGR gas temperature.

$$T_1 = \left(\frac{m_{egr}}{m_{egr} + w_{air}}\right) T_{em_{prev}} + \left(1 - \left(\frac{m_{egr}}{m_{egr} + w_{air}}\right)\right) T_{in} \qquad (3.)$$

3.1.2 Compression stroke

The air charge is compressed in this part of the cycle to reach ignition temperatures. The compression is modelled as an adiabatic process with fixed adiabatic coefficient gamma. In the model start of compression is when the piston is at the BDC and begins to move upwards to the TDC. The end of compression is assumed to occur at the TDC position of the piston. Assuming ideal gas laws for adiabatic compression, we can compute the final pressure and temperature of the gases in the system after compression.

$$\gamma_1 = \left(\frac{C_{p_1}}{C_{v_1}}\right) \qquad (4.)$$

$$P_2 = P_1 \left(\frac{V_1}{V_2}\right)^{\gamma} \qquad (5.)$$

$$T_2 = T_1\left(\frac{V_1}{V_2}\right)^{\gamma-1} \quad (6.)$$

Heat transfer is modelled after the compression is complete. The major fraction of heat lost is assumed to be lost through the walls of the cylinder and cylinder head. A single wall boundary is assumed for the gases. Using first law of thermodynamics, we can write a heat balance equation for the transfer of heat from the gases through the walls to the coolant. The coolant temperature is a measured signal in the control system. The wall temperature at this stage is assumed to be equal to the intake charge temperature. The coolant jacket around the cylinder sleeves and cylinder head act as a heat sink.

$$T_{w1} = T_1 \quad (7.)$$

$$m_1 = m_{egr} + w_{air} \quad (8.)$$

The Hohenberg equations are used to compute an overall heat transfer coefficient for the system.

$$h_g = C1 * (V1^{-0.06}) * \left(\left(\frac{P1}{100000}\right)^{0.8}\right) * (T1^{-0.4}) * (sp\ +\ C2)^{0.8} \quad (9.)$$

An energy balance is used to compute the temperature after heat transfer and then the new wall temperatures are computed.

$$T_{2_{ht}} * (m_1C_v + h_gA_g) = \ (m_1C_vT_2 + h_cA_gT_{w1}) \quad (10.)$$

$$T_{2_{ht}} = \frac{m_1C_vT_2 + h_cA_gT_{w1}}{(m_1C_v + h_gA_g)} \quad (11.)$$

$$T_{w2} * (h_gA_g + h_cA_g) = \left(h_gA_gT_{2_{ht}} + h_cA_cT_c\right) \quad (12.)$$

$$T_{w2} = \frac{\left(h_gA_gT_{2_{ht}} + h_cA_cT_c\right)}{(h_gA_g + h_cA_g)} \quad (13.)$$

3.1.3 Combustion

The combustion process in diesel engines is a process of heat release from the fuel over several crank angle degrees. In this modelling approach, we assume a lumped heat release from the entire quantity of the fuel injected into the system. Complete combustion is assumed for the fuel. Combustion is assumed to occur in two phases. The first phase is the constant volume combustion and the second phase is constant pressure combustion.

Constant volume combustion is characteristic feature of an ideal Otto Cycle. The combustion of the fuel in this phase occurs at constant volume. So the volume before and after the combustion remains the same. This stage simulates a sudden release of heat into the system from the fuel.

Constant volume combustion: Temperature, pressure and volume are computed for this stage of the system.

$$\left(T_{3a} - T_{2_{ht}}\right) * \left(w_{fuel} + w_{air} +\ m_{egr}\right)C_v = w_{fuel}x_{cv}q_{hc} \quad (14.)$$

$$T_{3a} = T_{2_{ht}} + inj\_corr\left(\frac{w_{fuel}x_{cv}q_{hc}}{\left(w_{fuel} + w_{air} +\ m_{egr}\right)C_v}\right) \quad (15.)$$

$$P_{3_a} = P_2\left(\frac{T_{3a}}{T_{2_{ht}}}\right) \quad (16.)$$

$$V_{3_a} = V_2 \quad (17.)$$

Heat transfer is modelled after the first phase of the combustion is complete. The total mass in the control system is the sum of the air mass, fuel mass and recirculated exhaust gases. The wall temperature is computed as a balance between the coolant temperature and the temperature of the gases after compression. Using first law of thermodynamics, we can write a heat balance equation for the transfer of heat from the gases through the walls to the coolant.

$$m_2 = w_{fuel}P_{fuel_{corr}}x_{cv} + w_{air} + m_{egr} \tag{18.}$$

Overall heat transfer coefficients are computed using the Hohenberg correlation.

$$h_{g1} = C1 * (V2^{-0.06}) * \left(\left(\frac{P2}{100000}\right)^{0.8}\right) * (T2_{ht})^{-0.4} * (sp\ +\ C2)^{0.8} \tag{19.}$$

The heat balance of the system gives us the final wall temperature and the temperature of gases after heat transfer.

$$A_g = A_p \tag{20.}$$

$$T_{3a_{ht}} * (m_2C_v + h_{g1}A_g) = m_2C_vT_{3a} + h_{g1}A_gT_{w2} \tag{21.}$$

$$T_{3a_{ht}} = \frac{m_2C_{v3a}T_{3a} + h_{g1}A_gT_{w2}}{(m_2C_{v3a} + h_{g1}A_g)} \tag{22.}$$

$$T_{w_{3a}} * (h_{g1}A_g + h_cA_c) = h_{g1}A_gT_{3a_{ht}} + h_cA_cT_c \tag{23.}$$

$$T_{w_{3a}} = \frac{h_{g1}A_gT_{3a_{ht}} + h_cA_cT_c}{(h_{g1}A_g + h_cA_c)} \tag{24.}$$

The fraction of the fuel that remains after the constant volume combustion, is assumed to undergo constant pressure combustion. Constant pressure combustion is characteristic feature of an ideal Diesel Cycle. The combustion of the fuel in this phase occurs at constant pressure. So the pressure before and after the combustion remains the same. This stage simulates an expanding gas mass that is a result of formation of gaseous species on combustion and the rapid expansion of these gases pushing the piston downwards.

Constant pressure combustion: Temperature, pressure and volume are computed for this stage of the system.

$$(T3 - T_{3a_{ht}}) * \left(w_{fuel} +\ w_{air} +\ w_{r_{prev}}\right)C_p = \left(w_{fuel}(1 -\ x_{cv})q_{hv}\right) \tag{25.}$$

$$T3 = T_{3a_{ht}} + \frac{\left(w_{fuel}\left(1 -\ P_{fuel_{corr}}x_{cv}\right)q_{hv}\right)}{(w_{fuel} +\ w_{air} +\ m_{egr})C_p} \tag{26.}$$

$$P_3 = P_{3a} \tag{27.}$$

$$V_3 = \frac{T_3V_{3a}}{T_{3a_{ht}}} \tag{28.}$$

Heat transfer is modelled after the second phase of the combustion is complete.

Overall HT coefficient post constant pressure combustion is computed. After which the heat balance gives final temperatures for the wall and the gas.

$$m_{3a} = w_{fuel} + w_{fuel} + m_{egr} \tag{29.}$$

$$h_{g2} = C1 * (V_{3a})^{-0.06}\ * \left(\left(\frac{P_{3a}}{100000}\right)^{0.8}\right) * \left(T_{3a_{ht}}\right)^{-0.4} * (sp\ +\ C2)^{0.8} \tag{30.}$$

$$T_{3_{ht}} * \left(m_{3a}C_{v3a} + h_{g2}A_g\right) = m_{3a}C_{v3a}T_3\ +\ h_{g2}A_gT_{w_{3a}} \tag{31.}$$

$$T_{3_{ht}} = \frac{m_{3a}C_{v3a}T_3\ +\ h_{g2}A_gT_{w_{3a}}}{\left(m_{3a}C_{v3a} + h_{g2} * A_g\right)} \tag{32.}$$

$$T_{w3} * \left(h_{g2}A_g + h_cA_c\right) = h_{g2}A_gT_{3_{ht}} + h_c * A_cT_c \tag{33.}$$

$$T_{w3} = \frac{h_{g2}A_gT_{3_{ht}} + h_cA_cT_c}{\left(h_{g2}A_g + h_cA_c\right)} \tag{34.}$$

3.1.4 Expansion

The exhaust gases in the cylinder begin to expand after the end of combustion, as the piston moves towards the BDC. In the model, this is assumed to be an adiabatic expansion for ideal gases. Similar to the compression phase, an adiabatic expansion coefficient gamma defines the characteristic expansion curve. The pressure and temperature of the gases is computed after the adiabatic expansion

$$Y_3 = c_{p_3} / c_{v_3} \tag{35.}$$

$$P_4 = P_3 * \left(\frac{V_3}{V_4}\right)^{Y_3} \tag{36.}$$

$$T_4 = T_{3_{ht}} \left(\frac{V_3}{V_4}\right)^{Y_3 - 1} \tag{37.}$$

Heat transfer is modelled after the expansion phase of the cycle is complete.
Over all HT coefficient post expansion is computed and the heat balance gives the final gas temperature.

$$h_{g_e} = C_1 * (V4 * -0.06) * \left(\left(\frac{P_4}{100000}\right)^{0.8}\right) * \left(T_{3_{ht}}\right)^{-0.4}) * \left(s_p \ + \ C_2\right)^{0.8} \tag{38.}$$

$$m_3 = w_{fuel} + w_{air} + m_{egr} \tag{39.}$$

$$Y_4 = \left(\frac{C_{p4}}{C_{v4}}\right) \tag{40.}$$

$$T_{4_{ht}} * (m_3 C_{v4} + h_g A_g) = m_3 C_{v4} T_4 \ + \ h_g A_g T_{w3} \tag{41.}$$

$$T_{4_{ht}} = \frac{m_3 C_{v4} T_4 \ + \ h_g A_g T_{w3}}{(m_3 C_{v4} + h_g A_g)} \tag{42.}$$

3.1.5 Flow through Exhaust Port

The exhaust gases flow through the exhaust port after coming out of the exhaust valve. The port is a metallic chamber surrounded by coolant jackets which act as a heat sink. The exhaust gases lose heat into the coolant through the port walls. A control volume is assumed in the port and an energy balance equation is used to compute the port wall temperature. After which the final energy balance of the control volume in the port is used to compute the exhaust gas temperature coming out of the port.

$$T_{w_{port}} * h_{g_{port}} A_{gw} + h_c A_{cw} = h_{g_{port}} A_{gw} T_4 + h_c A_{cw} T_c \tag{43.}$$

$$T_{w_{port}} = \left(\frac{h_{g_{port}} A_{gw} T_4 + h_c A_{cw} T_c}{h_{g_{port}} A_{gw} + h_c A_{cw}}\right) \tag{44.}$$

$$m_{port} = m_{flow} * egr_{corr} * (w_{air} + w_{fuel}) \tag{45.}$$

$$T_{modelled} * (m_{port} C_{p4} + h_{g_{port}} A_{gw}) = m_{port} C_{p4} T_{4_{ht}} + h_{g_{port}} A_{gw} T_{w_{port}} \tag{46.}$$

$$T_{modelled} = \left(\frac{m_{port} C_{p4} T_{4_{ht}} + h_{g_{port}} A_{gw} T_{w_{port}}}{m_{port} C_{p4} + h_{g_{port}} A_{gw}}\right) \tag{47.}$$

3.2 CAD resolved Model

This model is also a physical equation based model with computations being done along crank angle degrees. The resolution of these computations is every 10 crank angle degrees. The computations are done over 4 strokes of the piston and so covers one cycle of the four stroke compression ignition engine. All the steps of the Cycle are described below with the physical equations governing them. The pictorial representation of the cycle events along crank angle degrees is illustrated below *(Figure 16)*.

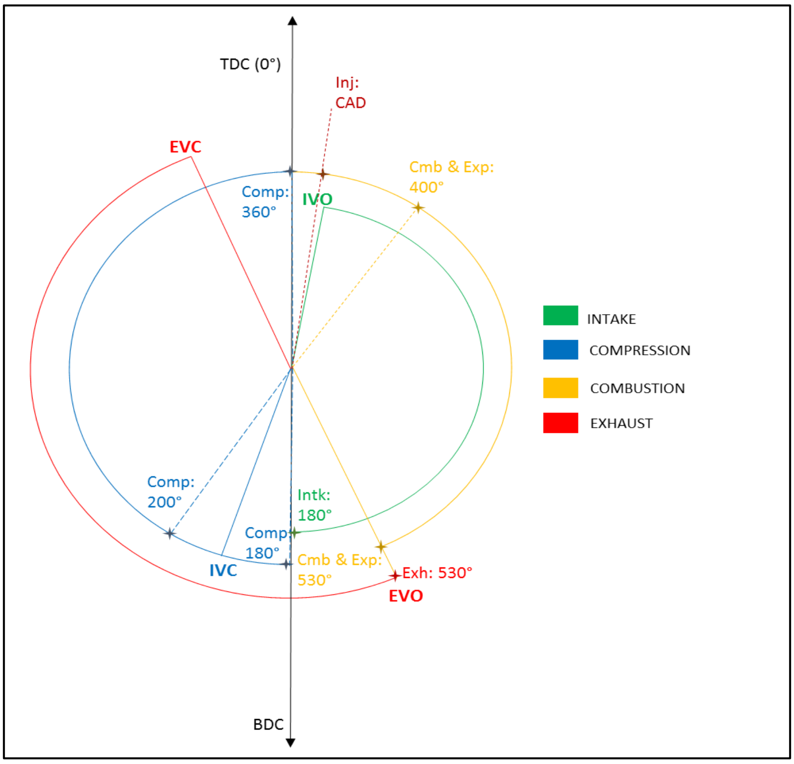

Figure 16 :- Illustration of valve events along Crank Angle Degrees in a 4 stroke Diesel cycle as implemented in the model.

3.2.1 Intake stroke

The fresh air charge is sucked in through the air filter and then finally reaches the intake manifold. The fresh charge is mixed with exhaust gases that are recirculated into the intake. The final temperature of the air charge is the balance between the temperature of the fresh air charge and the EGR gas temperature. This temperature is calculated for the end of the compression stroke. This is then used as the input gas temperature for the compression stroke. The temperature is computed at only one crank angle degree, i.e. at BDC since gas mixture temperature just before the start of compression is relevant for the model.

$$m1 = w_{air} + m_{egr} \tag{48.}$$

$$theta_{dur} = P_{fuel_{corr}} * 360 * \ comb_{dur} \left(\frac{mN}{1000}\right) \tag{49.}$$

$$\mathrm{T1_{ht(180)}} = \left(\frac{\mathrm{m_{egr}}}{\mathrm{m_{egr} + w_{air}}}\right) * \mathrm{T_4[dk]} + \left(1 - \left(\frac{\mathrm{m_{egr}}}{\mathrm{m_{egr} + w_{air}}}\right)\right) * \mathrm{T_{im}} \tag{50.}$$

$$P_{1_{(180)}} = P_1 \tag{51.}$$

3.2.2 Compression stroke

The air charge is compressed in this part of the cycle to reach ignition temperatures. The compression is modelled at crank angles (180,200 & 350) before the end of the compression stroke i.e. when the piston reaches the TDC. In this case also the process is assumed to be adiabatic with fixed adiabatic coefficient gamma. Assuming ideal gas laws for adiabatic compression, we can compute the final pressure and temperature of the gases in the system after compression. The gamma for the adiabatic compression is computed using the specific heats and the temperature & pressure are computed following that.

$$Y_{(180)} = \left(\frac{C_{p(180)}}{C_{v(180)}}\right) \tag{52.}$$

$$T_{1(200)} = T_{1(180)} * \left(\frac{V_{1(180)}}{V_{1(200)}}\right)^{Y_{180}-1} \quad (53.)$$

$$P_{1(200)} = P_{1(180)} * \left(\frac{V_{1(180)}}{V_{1(200)}}\right)^{Y_{180}} \quad (54.)$$

Using first law of thermodynamics, we can write a heat balance equation for the transfer of heat from the gases through the walls to the coolant. The coolant temperature is a measured signal in the control system. The wall temperature is also computed by energy balance. The coolant jacket around the cylinder sleeves and cylinder head act as a heat sink. Hohenberg heat transfer correlations are used to develop overall heat transfer coefficient for the process.

$$A_{c(200)} = A_{g\,(200)} \quad (55.)$$

$$h_{g_{cmp(200)}} = swirl_{corr} * C_1 * \left(V_{1(200)}\right)^{-0.06} * \left(\left(\frac{P_{1(200)}}{100000}\right)^{0.8}\right) * \left(T_{1(200)}\right)^{-0.4} * (sp + C_2)^{0.8} \quad (56.)$$

$$T_{w1(200)} = \frac{\left(h_{g_{cmp(200)}} * A_{g\,(200)} * T_{1(200)} + h_c * A_{c(200)} * T_c\right)}{h_{g_{cmp(200)}} * A_{g\,(200)} + h_c * A_{g\,(200)}} \quad (57.)$$

$$Y_{200} = \left(\frac{Cp_{200}}{Cv_{200}}\right) \quad (58.)$$

$$T_{1_{ht(200)}} = \frac{m_1 * Cv_{(200)} * T_{1(200)} + h_{g_{cmp(200)}} * A_{g\,(200)} * T_{w1(200)}}{m_1 * Cv_{(200)} + h_{g_{cmp(200)}} * A_{g\,(200)}} \quad (59.)$$

The computations for 200 crank angle degree are repeated for the CAD 350, i.e. 10 degrees before TDC.

3.2.3 Combustion

The combustion process in diesel engines is a process of heat release from the fuel over several crank angle degrees. In this modelling approach, we create a heat release profile with dependency on the crank angle degrees. Complete combustion is assumed for the fuel. Only the fuel in the main injection is considered to be contributing to the heat release process.

Temperature computed after compression to 350 CAD,

$$T_{1(350)_c} = T_{1(200)_{ht}} * \left(\frac{V_{1(200)}}{V_{1(350)}}\right)^{Y_{200}-1} \quad (60.)$$

Wiebe Function is used to develop a rate of heat release curve for each operating point. This is done by tuning the various parameters of the Wiebe function. Combustion duration for each operating point is optimized. The reference values for combustion duration are taken from Heywood [1]. The combustion duration can be seen to range from 6 to 10 Ms. The combustion duration is modelled as a function of fuel quantity available for combustion and is monotonically increasing with increase in fuel quantity. Since the engine speed is known at each operating point, we can calculate the crank angle duration for the combustion.

$$delta_{theta_{(350)}} = theta_{(350)} * \left(\frac{180}{\pi}\right) - (360 + inj_{tim_c}) \quad (61.)$$

While using the Wiebe function, the parameters M1 and M2 are tuned so as to accommodate other effects in the combustion process. The values for these parameters are kept constant for all operating points and are not optimized for individual points. This is to keep the shape of the heat release curve consistent. X_b i.e. the fraction of fuel burnt at a given crank angle is computed. The mass fraction and successively total mass of fuel burnt at 350 CAD is computed using the Wiebe function,

$$x_{b_{350}} = \left(1.0 - exp\left(-M_1 * \left(\frac{delta_{theta\_positive_{(350)}}}{theta_{dur}}\right) ** (M_2 + 1)\right)\right) \quad (62.)$$

$$fuel_{br_{350}} = w_{fuel} * x_{b_{350}} \quad (63.)$$

This fuel quantity is used to compute the heat release in the system on complete combustion of the injected fuel at this crank angle. The heat release results in increased temperature and pressure of the gas in the system which is further computed.

$$T_{1_{350}} = T_{1_{350c}} + \frac{fuel_{br_{350}} * q_{h_v}}{(fuel_{br_{350}} + w_{air} + m_{egr}) * \left(c_{p_{(180)}}\right)} \quad (64.)$$

$$P_{1_{(350)}} = P_{1_{(200)}} * \left(\frac{V_{1_{(200)}}}{V_{1_{(350)}}}\right)^{Y(200)} \quad (65.)$$

The overall heat transfer coefficient is computed using Hohenberg correlations to obtain final wall and gas temperatures after the combustion at this crank angle degree is complete.

$$m_{1_{(350)}} = w_{air} + fuel_{br_{350}} + m_{egr} \quad (66.)$$

$$h_{g_{cmb350}} = C_1 * (V_{1_{350}})^{-0.06} * \left(\left(\frac{P_{1_{350}}}{100000}\right)^{0.8}\right) * (T_{1_{350}})^{-0.4} * (s_p + C_2)^{0.8} \quad (67.)$$

$$T_{w1_{350}} = \frac{h_{g_{cmb(350)}} * A_{g_{(350)}} * T_{1_{(350)}} + h_c * A_{c_{(350)}} * T_c}{h_{g_{cmb(350)}} * A_{g_{(350)}} + h_c * A_{c_{(350)}}} \quad (68.)$$

$$Y_{(350)} = Cp_{(350)}/Cv_{(350)} \quad (69.)$$

$$T_{1_{(350)ht}} = \frac{m_{1_{(350)}} * Cv_{(350)} * T_{1_{(350)}} + h_{g_{cmb(350)}} * A_{g_{(350)}} * T_{w1_{(350)}}}{m_{1_{350}} * Cv_{(350)} + h_{g_{cmb350}} * A_{g_{350}}} \quad (70.)$$

Computation for the next CAD angle i.e. 360 follows. The fuel injected between the previous and the current crank angle degree contributes to the increase in temperature and pressure of the system which is computed using the equations similar preceding equations.

Temperature computed after compression to 360 CAD,

$$T_{1_{(360)_c}} = T_{1_{(350)_{ht}}} * \left(\frac{V_{1_{(350)}}}{V_{1_{(360)}}}\right)^{Y_{200}-1} \quad (71.)$$

$$delta_{theta_{(360)}} = theta_{(360)} * \left(\frac{180}{\pi}\right) - (360 + inj_{tim_c}) \quad (72.)$$

The mass fraction and successively total mass of fuel burnt at 360 CAD is computed using the Wiebe function,

$$x_{b_{360}} = \left(1.0 - exp\left(-M_1 * \left(\frac{delta_{theta\_positive_{(360)}}}{theta_{dur}}\right) ** (M_2 + 1)\right)\right) \quad (73.)$$

$$fuel_{br_{360}} = w_{fuel} * x_{b_{350}} - fuel_{br_{350}} \quad (74.)$$

This fuel quantity is used to compute the heat release in the system on complete combustion of the injected fuel at this crank angle. The heat release results in increased temperature and pressure of the gas in the system which is further computed.

$$T_{1_{360}} = T_{1_{360c}} + \frac{fuel_{br_{360}} * q_{h_v}}{(fuel_{br_{360}} + w_{air} + m_{egr}) * \left(c_{p_{(350)}}\right)} \quad (75.)$$

$$P_{1_{(360)}} = P_{1_{(350)}} * \left(\frac{V_{1_{(350)}}}{V_{1_{(360)}}}\right)^{Y_{(350)}} \quad (76.)$$

The overall heat transfer coefficient is computed using Hohenberg correlations to obtain final wall and gas temperatures after the combustion at this crank angle degree is complete.

$$m_{1_{(360)}} = w_{air} + fuel_{br_{360}} + m_{egr} \quad (77.)$$

$$h_{g_{cmb_{360}}} = C_1 * (V_{1_{360}})^{-0.06} * \left(\left(\frac{P_{1_{360}}}{100000}\right)^{0.8}\right) * (T_{1_{360}})^{-0.4} * (s_p + C_2)^{0.8} \quad (78.)$$

$$T_{w1_{360}} = \frac{h_{g_{cmb(360)}} * A_{g_{(360)}} * T_{1_{(360)}} + h_c * A_{c_{(360)}} * T_c}{h_{g_{cmb(360)}} * A_{g_{(360)}} + h_c * A_{c_{(360)}}} \quad (79.)$$

$$Y_{(360)} = Cp_{(360)}/Cv_{(360)} \quad (80.)$$

$$T_{1_{(360)ht}} = \frac{m_{1_{(360)}} * Cv_{(360)} * T_{1_{(360)}} + h_{g_{cmb(360)}} * A_{g_{(360)}} * T_{w1_{(360)}}}{m_{2_{360}} * Cv_{(360)} + h_{g_{cmb_{360}}} * A_{g_{360}}} \quad (81.)$$

The same computations are continued at a resolution of every 10 crank angle degree, till the exhaust valves open.

3.2.4 Expansion

The exhaust gases in the cylinder begin to expand after the end of combustion, as the piston moves towards the BDC. In the model, this is assumed to be an adiabatic expansion for ideal gases. In case the injection starts after the piston moves down from the TDC, the gases in the cylinder expand adiabatically. This delay in injection leads to an expansion of the gases before combustion start which is also included in the model.

The computations for heat release also continue along with the expansion. The pressure and temperature increase due to expansion along crank angle degrees is optimized using correction factors.

The discussed phenomenon are reflected in crank angle degrees after TDC and continue till exhaust valve opening.

$$delta_{theta_{(430)}} = theta_{(430)} * \left(\frac{180}{\pi}\right) - (360 + inj_{tim\_c}) \quad (82.)$$

$$x_{b_{430}} = \left(1.0 - exp\left(-M_1 * \left(\frac{delta_{theta\_positive_{(430)}}}{theta_{dur}}\right) ** (M_2 + 1)\right)\right) \quad (83.)$$

$$fuel_{br_{430}} = w_{fuel} * x_{b_{430}} - fuel_{br_{420}} \quad (84.)$$

$$T_{2_{430}} = T_{2_{420ht}} + \frac{fuel_{br_{430}} * q_{h_v}}{(fuel_{br_{430}} + w_{air} + m_{egr}) * \left(c_{p_{(420)}}\right)} \quad (85.)$$

$$P_{2_{430}} = P_{inj} \quad (86.)$$

$$T_{2e_{(430)}} = T_{em_{corr}} * T_{2_{(430)}} * \left(\frac{V_{2_{(420)}}}{V_{2_{(430)}}}\right)^{Y_{(420)}-1} \quad (87.)$$

$$P_{2e_{(430)}} = P_{em_{corr}} * P_{2_{(430)}} * \left(\frac{V_{2_{(420)}}}{V_{2_{(430)}}}\right)^{Y_{(420)}} \quad (88.)$$

$$m_{2_{(430)}} = w_{air} + fuel_{br_{430}} + m_{egr} \quad (89.)$$

$$A_{c_{430}} = A_{g_{430}} \quad (90.)$$

$$h_{g_{cmb430}} = C_1 * \left(V_{2_{430}}\right)^{-0.06} * \left(\left(\frac{P_{2e_{430}}}{100000}\right)^{0.8}\right) * \left(T_{2e_{430}}\right)^{-0.4} * \left(s_p \; + \; C_2\right)^{0.8} \quad (91.)$$

$$T_{w2_{(430)}} = \frac{h_{g_{cmb(430)}} * A_{g_{(430)}} * T_{2_{(430)}} + h_c * A_{c_{(430)}} * T_c}{h_{g_{cmb(430)}} * A_{g_{(430)}} + h_c * A_{c_{(430)}}} \quad (92.)$$

$$Y_{(430)} = Cp_{(430)}/Cv_{(430)} \quad (93.)$$

$$T_{2_{(430)ht}} = \frac{m_{2_{(430)}} * Cv_{(430)} * T_{2e_{(430)}} \; + \; h_{g_{cmb(430)}} * A_{g_{(430)}} * T_{w2_{(430)}}}{m_{2_{430}} * Cv_{(430)} + h_{g_{cmb430}} * A_{g_{430}}} \quad (94.)$$

The computations follow at every 10 crank angle degree till the exhaust valve opens.

3.2.5 Exhaust

The exhaust valve opening leads to the flow of exhaust gases through the exhaust port. A control volume assumed in the port and an energy balance is used to compute the wall temperatures of the port and the final gas temperatures after flow through the port.

$$T_{w_{port}} = \frac{h_{g_{port}} * A_{g_w} * T_{2_{(530)}} + h_c * A_{c_w} * T_c}{h_{g_{port}} * A_{g_w} + h_c * A_{c_w}} \quad (95.)$$

$$m_{port} = \; egr_{corr} * m_{flow} * (w_{air} + w_{fuel} + m_{egr}) \quad (96.)$$

The modelled exhaust gas temperature is finally computed at the end of the exhaust port after heat loss to the surrounding port walls.

$$T_{modelled} = \frac{m_{port} * c_{p_4} * T_{2_{(530)ht}} + h_{g_{port}} * A_{g_w} * T_{w_{port}}}{m_{port} * C_{p_4} + h_{g_{port}} * A_{g_w}} \quad (97.)$$

The error between the modelled and the measured temperature is minimized by optimizing the tuneable parameters in them model.

$$err_{abs} = T_{modelled} - T_{measured} \quad (98.)$$

4. Model Tuning

4.1 Test data

The test data available from previous tests in different engines are used to tune the models. The control system signals available from the test rigs are used as input to the model. The objective is to be able to use control system signals from the production ready engines. The test data recorded was for different operating points with specific variations in engine parameters. The types of test data recorded are discussed in following sections.

4.1.1 Focused tests

The test performed under this category had specific parameter variations. Four different data sets were used individually to tune the model. The variations in each dataset is as follows:

1. EGR system 1: First system of exhaust gas recirculation
2. EGR system 2: Second system for exhaust gas recirculation
3. Turbo Actuation: Variation in turbocharger parameters
4. Swirl Actuation: variation of pre-combustion Swirl

The final tuning of the model is done by the combined data from all four above data sets. This leads to improved calibration of the model.

The test data however available in this category has some transient characteristics. The model predicts steady state values for the exhaust temperature. But the measurement of the temperature at the engine test rig is done in short intervals. The operating points may switch from a high load condition to a low load condition very quickly. The sensor element of the probe and the wall temperatures change at a slower rate and so the transience of the signal leads to improper data recording. This does not reflect the steady state operating condition of the engine. The same is illustrated in the figure below *(Figure 17)*.

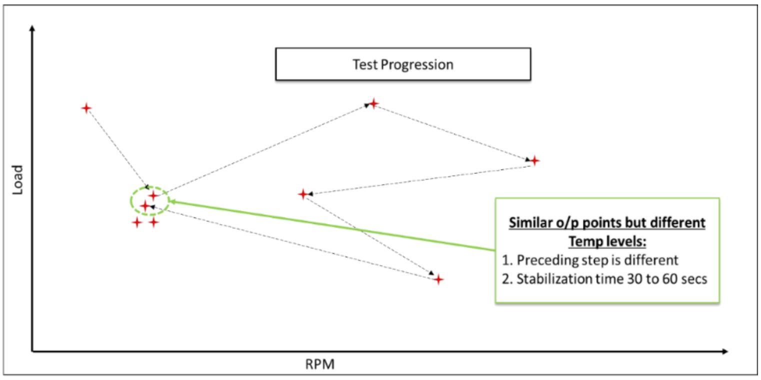

Figure 17:- Sample Engine dynamometer Test progression along various operating points, for focussed tests.

The cluster of points in a localized operating region should end up at similar steady state temperature values. But often this might not be the case. If the preceding step of a point in the cluster was a high load point then the temperature levels in the system are high.

4.1.2 Part load tests

The part load testing of the engine gives us a different data set for the model tuning. This data is closer to a steady state operating condition of the engine. There are three such data sets used in this category:

1. Part Load Test 1
2. Part Load Test 2
3. Part Load Test 3

The combined data of all the three data sets is used to tune the model. The tuned parameters of the model were calibrated to achieve improved accuracy of the exhaust temperature model.

4.2 Dual Cycle model tuning

The model has several parameters which depends on other factors. In order to compensate for these factors, we tune the model parameters. The following parameters in the model were tuned. For visualization of the parameter tuning, parameters from one of the data set is plotted after the description.

The heat transfer coefficient of the coolant, *hc* is tuned to get an optimized value for the dataset *(Figure 18)*. The coolant flow in the sleeves around the cylinder and the cylinder head keep varying based on the water pump speed. The water pump being coupled to the crankshaft runs at a speed proportional to the engine speed. Heat carrying capacity of the coolant is dependent of the flow characteristics, which in turn depends on the speed of the engine. Hence the correction factor of coolant heat transfer coefficient is tuned as a function of the engine speed.

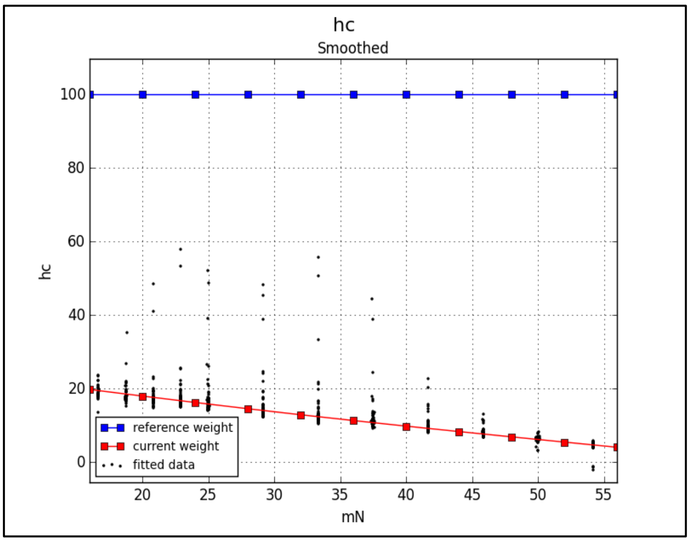

Figure 18 :- Tuned Heat transfer coefficient of coolant. X- Engine speed (rps).

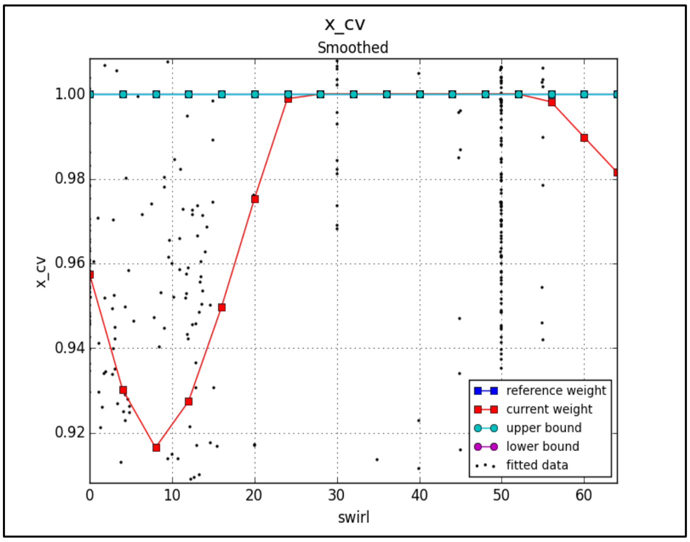

Figure 19 :- Y-Fuel fraction burnt at constant volume. X- Swirl value.

The mass of fuel burned at constant volume, *x_cv* is adjusted to get a more accurate heat release as it shown in *(Figure 19)*. The heat is ideally released as a function of the crank angle degrees. In the model, we assume complete heat release from the fuel. This effect results in a different temperature at end of combustion. So *x_cv* helps define the fraction of injected fuel burnt at constant volume. The remaining quantity is combusted at constant pressure.

The adiabatic expansion coefficient, gamma (γ_e) is indirectly tuned by tuning the specific heats. The temperature of the gases after the end of combustion are much higher than at intake. The specific heat values at constant pressure and constant volume are dependent on temperature and as a result an effective gamma value for this temperature range is computed by this model. The temperature dependency curves of specific heats are obtained from previous simulations.

Effective area of heat transfer from gas to the port walls, *Ag_w* is a parameter that is tuned in the model within constraints. The area available for heat transfer can vary based on the piston position and due to possible existence of hot and cold temperature zones in the system as it shown in *(Figure 20)*.

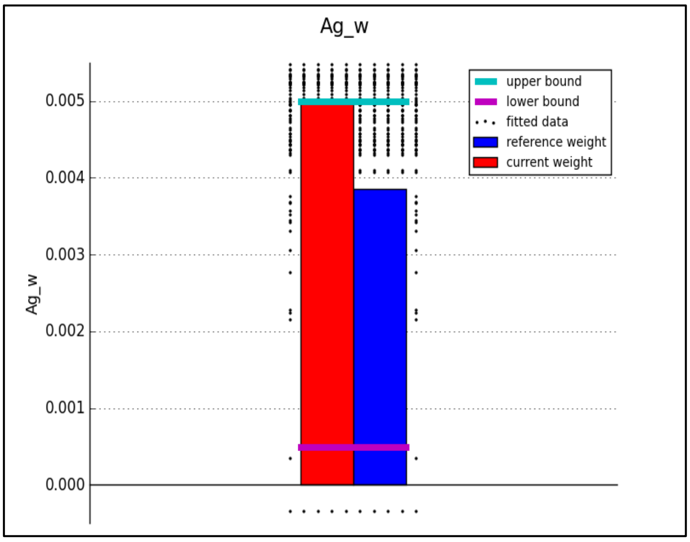

Figure 20 :- Effective area of heat transfer from gas to port walls. Optimized constant.

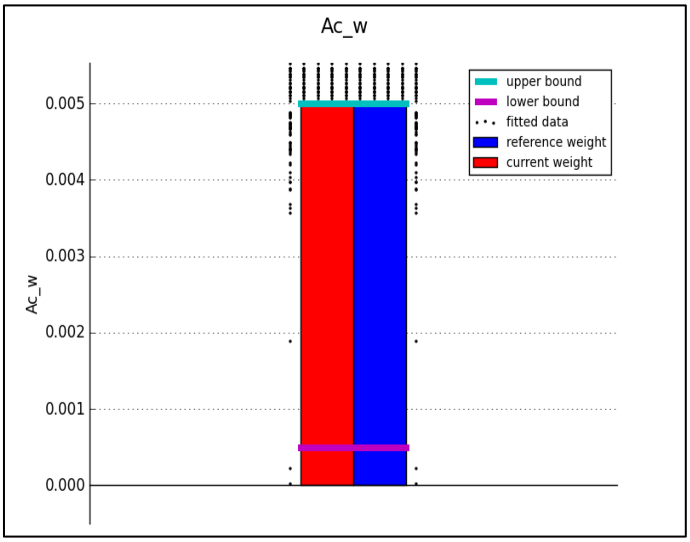

Figure 21 :- Effective area of heat transfer from port walls to coolant. Optimized constant.

Effective area of heat transfer from port walls to the coolant, *Ac_w* is a parameter that is tuned in the model within constraints *(Figure 21)*. The area available for heat transfer can vary based on the piston position and due to possible existence of hot and cold temperature zones in the coolant flow.

Hohenberg coefficient *C1* and *C2* are tuned parameters that take into account, factors that may result in a different value of heat transfer *(Figure 22)*. Factors like swirl turbulence or local ignitions and others.

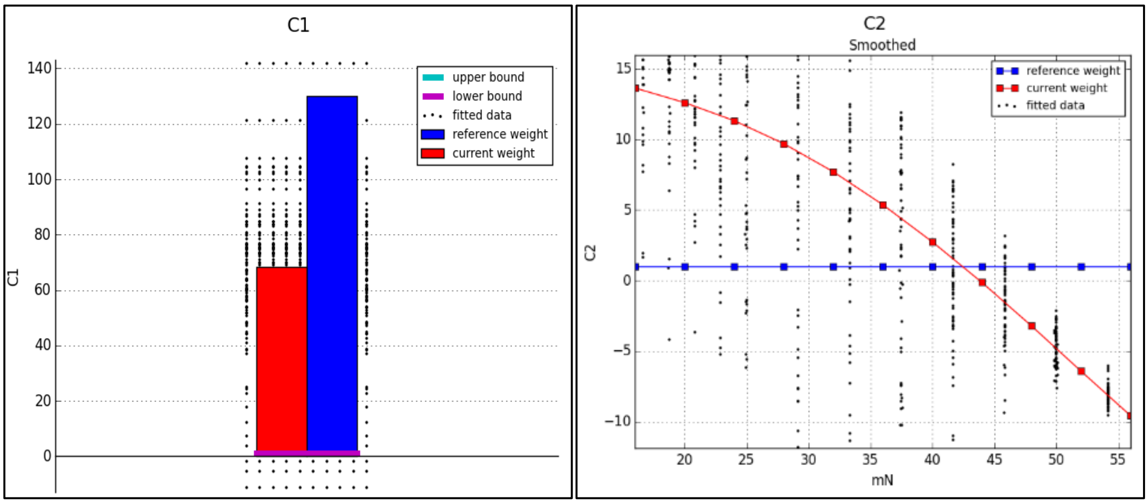

Figure 22 :- Left - Hohenbegr coefficient 1. Optimized constant. Right- Hohenberg coefficient 2, X- Engine speed (rps)

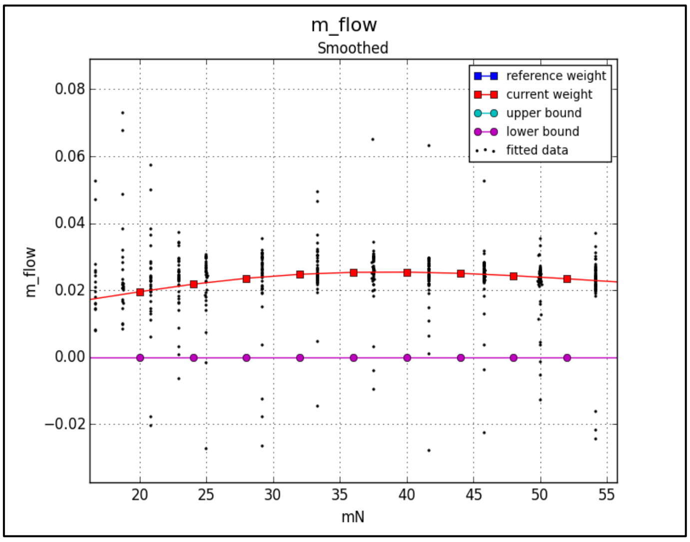

Figure 23 :- Mass correction in port control volume, X- Engine speed (rps)

Mass flow rate of the gases *m_flow* through the exhaust port influences the effective mass of the gas in the control volume *(Figure 23)*. This is corrected by calibrating it with the engine speed.

Heat transfer coefficient in the exhaust port *ht_port* is a tuned parameter. This varies with increased flow characteristics like turbulence and it is tuned with respect to the engine speed and it can be seen in *(Figure 24)*.

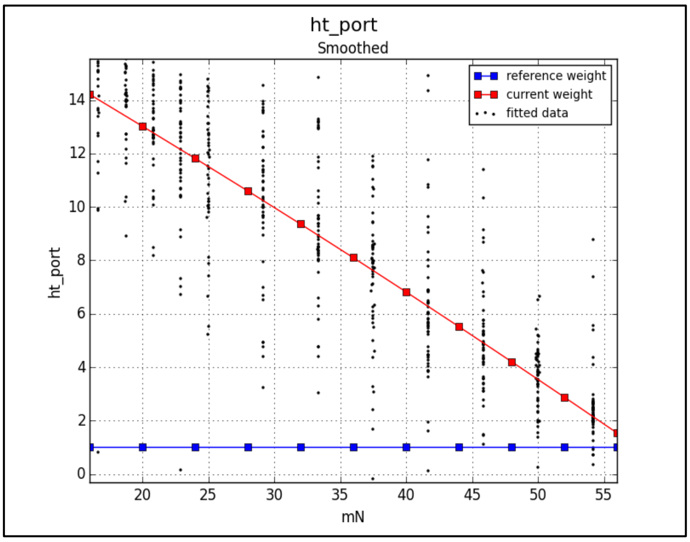

Figure 24 :- Heat transfer coefficient of gas in the exhaust port, X- Engine speed (rps)

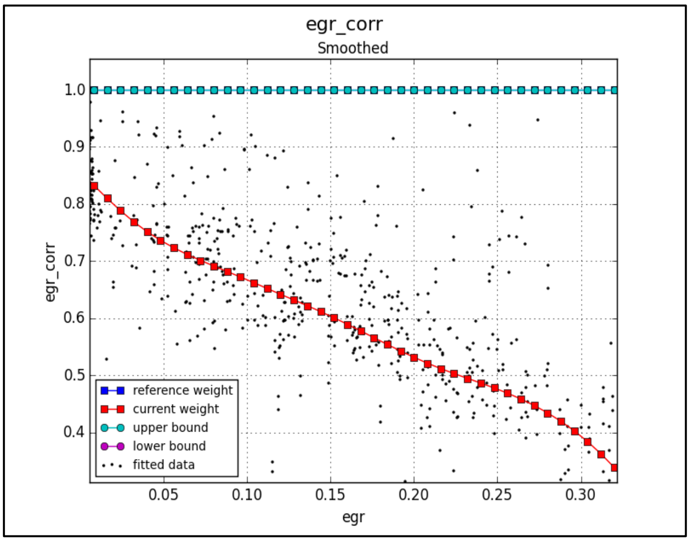

Figure 25 :- EGR mass correction, X- EGR fraction

The mass of gas flowing through the control volume in the exhaust port may vary based of the flow behavior in the port. The EGR gas mass being recirculated in the cylinder can influence the flow behavior in the port. As a compensation to this effect, an *egr_corr* factor is used while computing mass of gas in the control volume of exhaust port *(Figure 25)*. With increase of exhaust recirculation, the mass in the port control volume decreases.

The start of main injection determines beginning of heat release from the fuel. The dual cycle approach does not take this into account. To compensate for the injection timing, a factor *inj_corr* is used. This is a compensation on the temperature computation after beginning of heat release and can be illustrated in *(Figure 26)*.

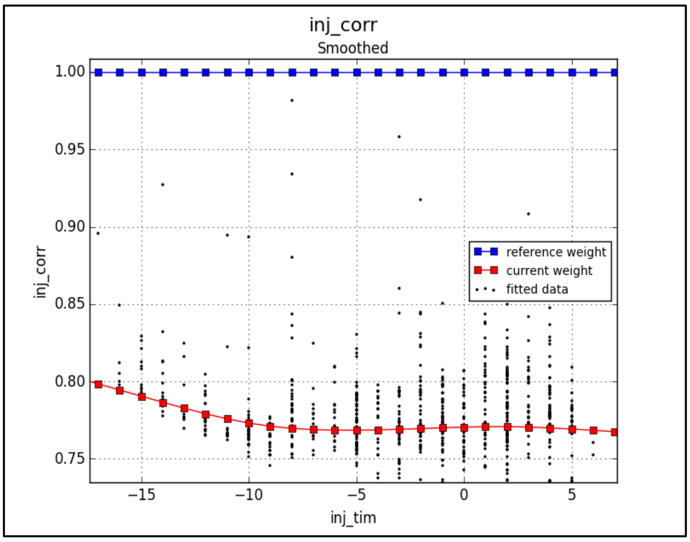

Figure 26 :- Correction factor for injection timing, X- Inject start Crank angle Degree

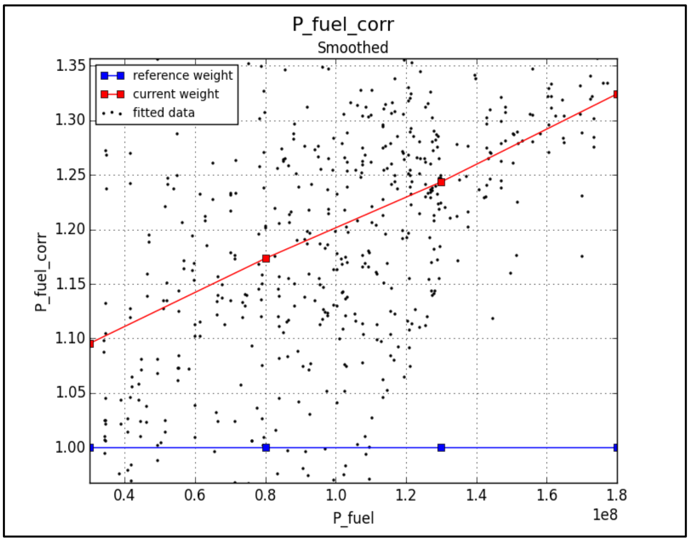

Figure 27 :- Correction of fuel mass fraction burnt based on fuel pressure, X- Fuel injection pressure.

The fuel pressure during injection influences the spray pattern and the combustion delay. This effect is factored in by using the correction *P_fuel_corr*. The factor is used in the computation of the mass fraction burned during constant pressure and mass fraction burned during constant volume combustion. Increasing fuel injection pressure leads to higher value for the factor *(Figure27)*.

4.3 Assumptions in Dual Cycle Model

The intake closes a few crank angle degrees after the BDC. During this period as the piston moves up, the air charge can be expelled out instead of getting compressed. But an ideal situation is assumed and this effect is ignored.

The fuel is sprayed into the air charge before the piston has reached the TDC. This results in charge cooling effect as the atomized fuel evaporates utilizing the heat from the air charge. This effect is also not taken into consideration.

All of the fuel is assumed to be combusted. This might not occur due to several related factors. The amount of heat release would thereby differ from the modelled value.

The dual cyclic behavior of the 4 strokes is not the case in a real engine. This dual cycle approach is still a close approximation and therefore used as a basis for this model. Part of the fuel is assumed to burn at constant pressure and the rest at constant volume.

Heat transfer in the port is computed by using one single control volume. This averaged computation leads to loss of some accuracy and can be improved by considering several other control volumes. The area available for heat transfer is assumed to constant and is equal to the area of the cylinder bore surface.

The geometric compression ratio is assumed constant for computation purposes. But the actual compression ratios may vary over time due to deposits and incompressible particles in the cylinder.

Valve events influencing the flow and mixing are compensated by correction factors and are not physically modelled.

4.4 CAD Resolved Model Tuning

The model has several parameters which are dependencies on other factors. In order to compensate for these factors, we need to tune the model parameters. The following parameters in the model were tuned. For better visualization of the parameter tuning, parameters from one of the data set is plotted after the description.

The time taken for combustion of the injected fuel, *comb_dur* is a tuned parameter. It is dependent on the amount of fuel injected in the main injection pulse. This is incremental with increasing fuel injection since it takes more time to combust a larger mass of fuel. The combustion duration is optimized for all operating points to develop a curve which captures the monotonic increase. Effect of tuned parameter *comb_dur* can be seen in given illustrated *(Figure 28)*.

The Wiebe curve parameters *M1* & *M2* are optimized for the entire data set resulting in one optimized set of values representing the shape of the curve and it can be seen in (*Figure 29)*.

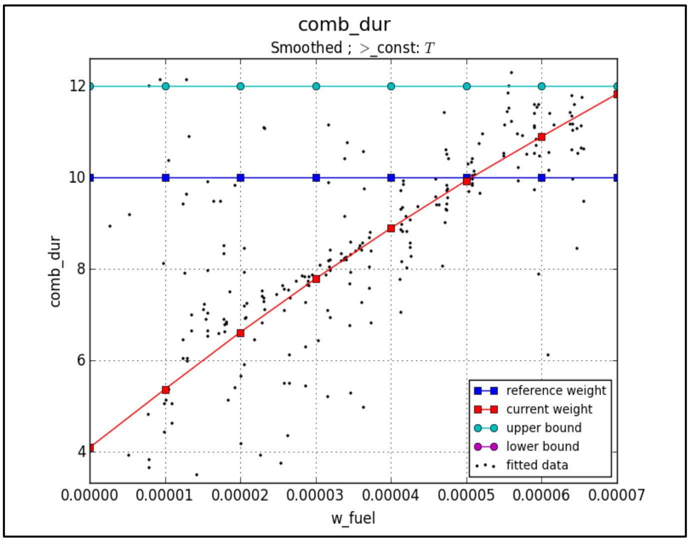

Figure 28 :- Tuned combustion duration based on fuel quantity injected, X- Fuel injected (Kg/stroke)

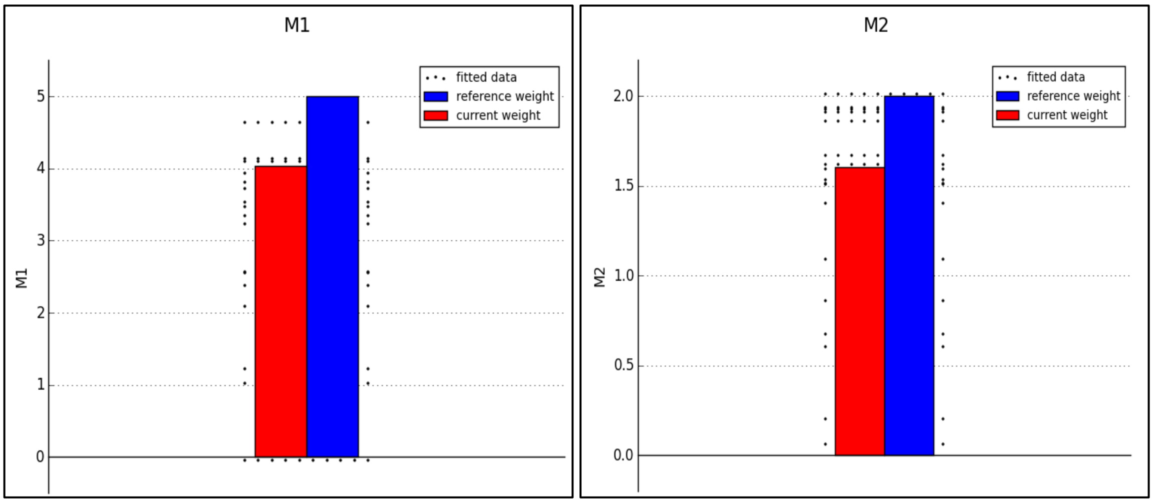

Figure 29 :- Optimized constant, Wiebe curve parameter 1 and 2

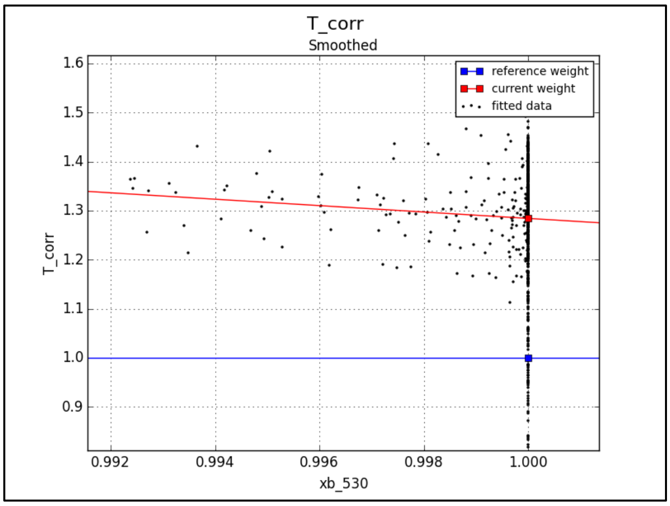

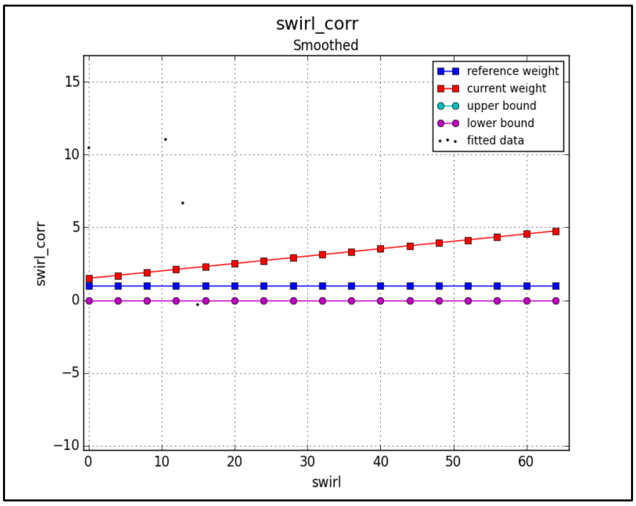

Figure 30 :- Temperature correction for unburnt fuel quantity. X- Mass fraction of fuel burnt at CAD 530 Figure 31 :- Heat transfer coefficient correction due to swirl. X- Swirl induced.

The rate of heat release might be such that the entire mass of fuel is not burnt within the modelled number of crank angle degrees. To add the effect of this remaining fraction of fuel a correction factor *T_corr* is introduced which is illustrated in *(Figure 30)*. This does not increase the temperature if the fuel fraction remaining at the last modelled crank angle degree is zero. For other cases, the temperature is compensated by this correction factor.

The swirl in the fresh charge is adjusted by mechanical actuation in the intake manifold. This results in different flow characteristics, different charge mixing and ultimately different levels of heat transfer effects. This is compensated in the compression part of the model where the factor *swirl_corr* is used as a product to the overall Hohenberg heat transfer coefficient. This factor is optimized for each operating point with a dependency on the mechanical actuation of the swirl valve. Effect of *swirl_corr* is represented in *(Figure 31)*.

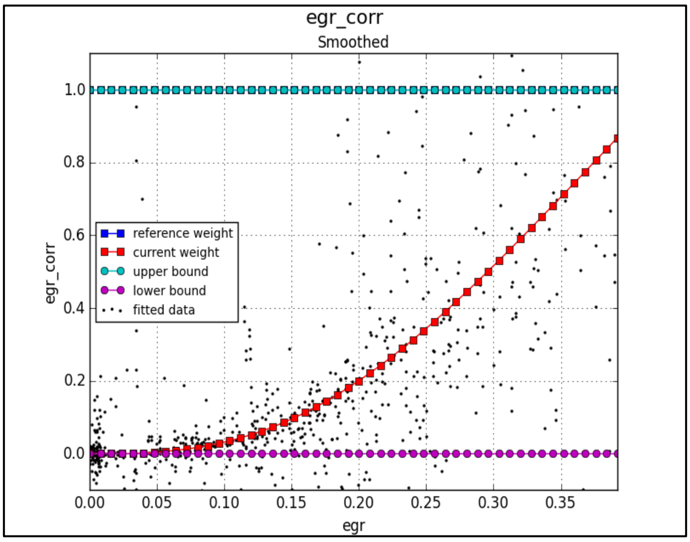

Figure 31 :- EGR quantity correction. X- EGR ratio

The correction factor *egr_corr* is multiplied to the mass of EGR flowing into the intake to mix with fresh charge. This is optimized for each operating point and is dependent on the estimated EGR flow ratio after sensor correction *(Figure 32)*.

The heat transfer coefficient of the coolant, *hc* is tuned to get a final heat transfer coefficient for the coolant *(Figure 33)*. The coolant flow in the sleeves around the cylinder and the cylinder head keep varying based on the water pump speed. The water pump being coupled to the crankshaft runs at a speed proportional to the engine speed. Heat carrying capacity of the coolant is dependent of the flow characteristics, which in turn depends on the speed of the engine. Hence the correction factor of coolant heat transfer coefficient is a function of the engine speed.

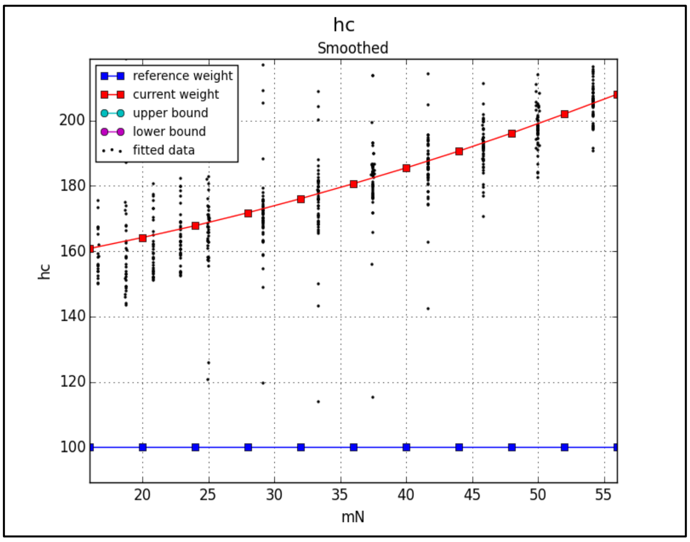

Figure 32 :- Tuned heat transfer coefficient of coolant. X- Engine speed (rps)

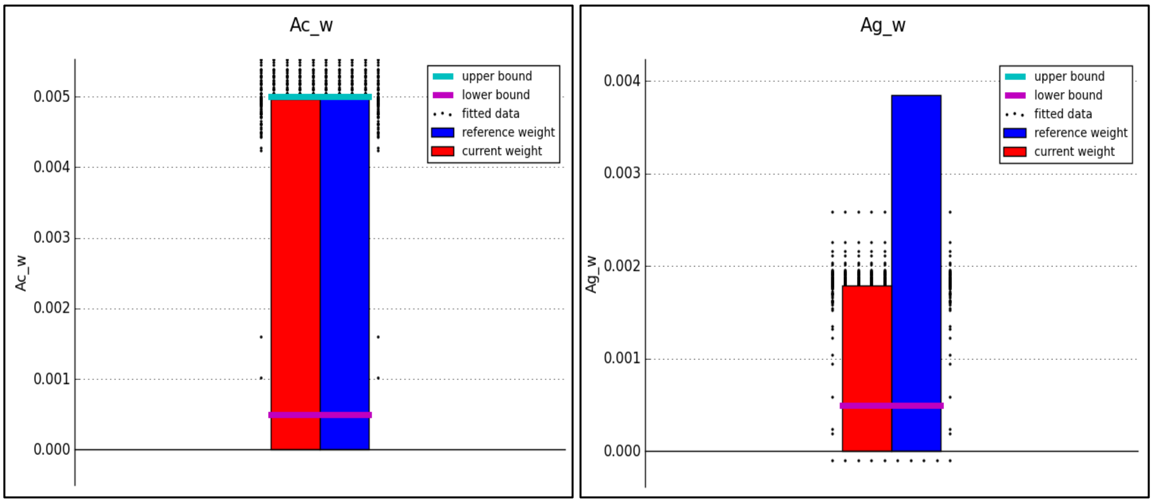

Figure 33 :- Left- Effective area of heat transfer from coolant to port walls. Right - Effective area of heat transfer from gas to port walls.

The adiabatic expansion coefficient, gamma (γ_e) is a tuned parameter. The temperature of the gases after the end of combustion are much higher. The specific heat values at constant pressure and constant volume are dependent on temperature and as a result an effective gamma value for this temperature range is computed by this model.

Effective area of heat transfer from gas to the port walls, *Ag_w* is a parameter that is tuned in the model within constraints *(Figure 34)*. The area available for heat transfer can be varying based on the piston position and the temperature zones in the system. The area available for heat transfer can be varying based on the piston position and the temperature zones in the coolant flow.

Hohenberg coefficient *C1* and *C2* are tuned parameters that take into account, factors that may result in a different value of heat transfer *(Figure 35)*. *C2* is optimized for each operating point and is dependent on the piston speed acting as a correction factor to the piston speed term in the Hohenberg equation for overall heat transfer coefficients.

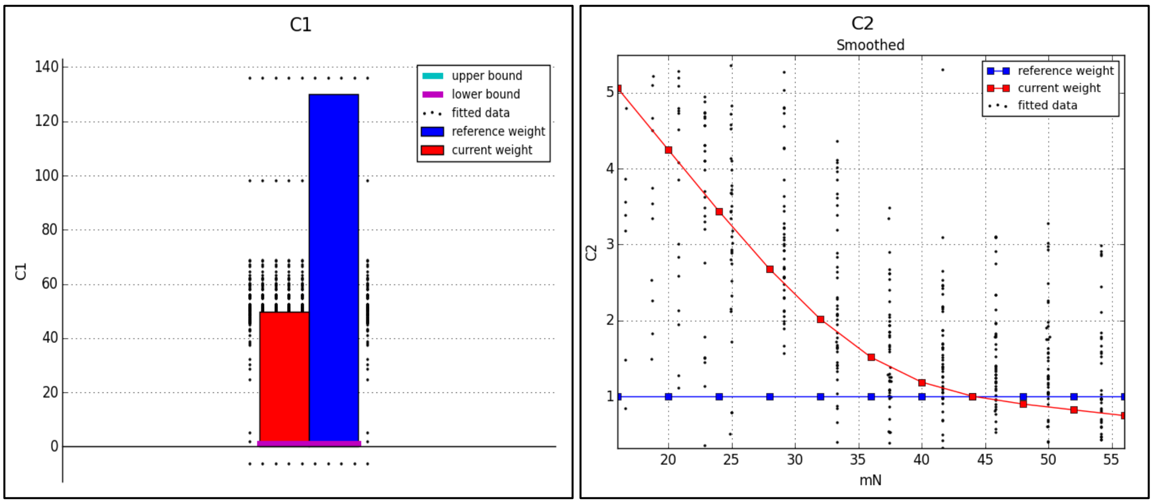

Figure 34 :- Left - Hohenberg coefficient 1. Optimized constant. Right- Hohenberg coefficient 2, X- Engine speed (rps)

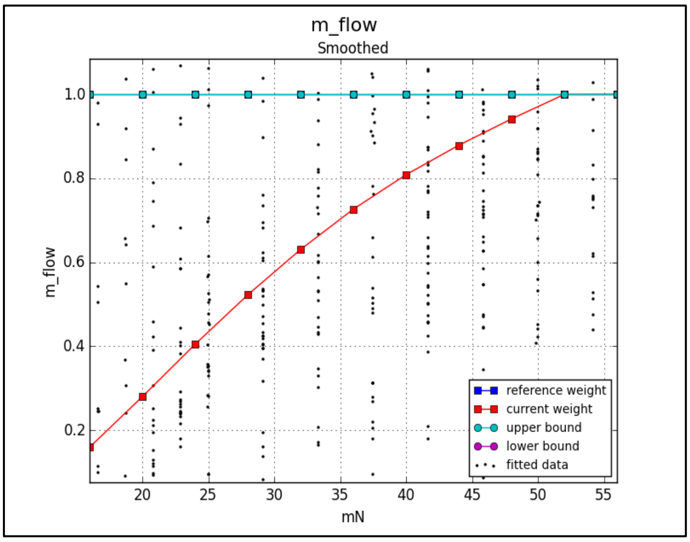

Figure 35 :- Mass correction in port control volume, X- Engine speed (rps

Mass flow rate of the gases *m_flow* through the exhaust port influences the effective mass of the gas in the control volume. This is corrected by calibrating it with the engine speed *(Figure 36)*.

Heat transfer coefficient in the exhaust port *hg_port* is a tuned parameter. This varies with increase flow characteristics like turbulence and it is tuned with respect to the air flow control signal acquired from the mass air flow sensor. This is representative of the gas mass flow through the exhaust *(Figure 37)*.

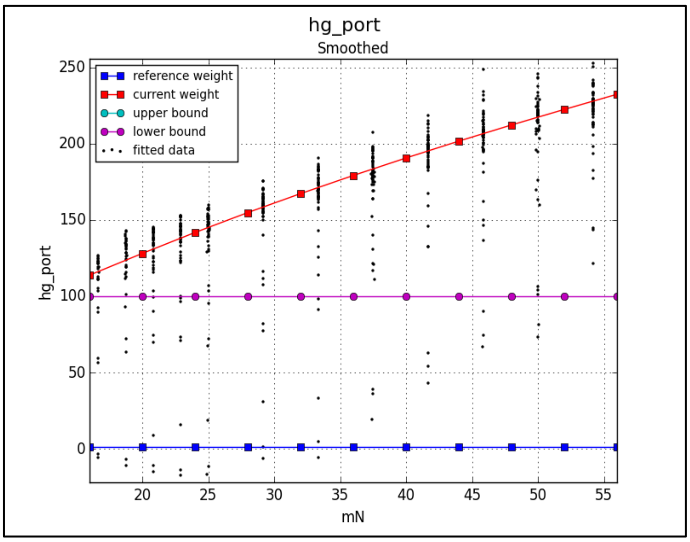

Figure 36 :- Heat transfer coefficient of gas in the exhaust port, X- Engine speed (rps)

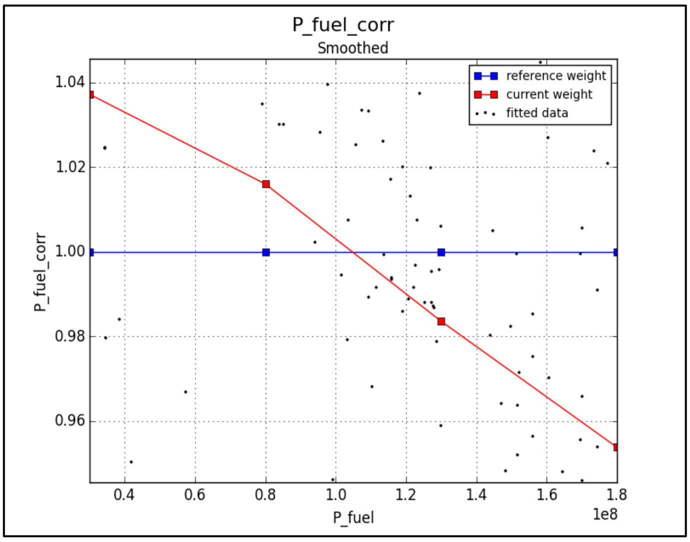

Figure 37 :- Correction of fuel mass fraction burnt based on fuel pressure, X- Fuel injection pressure.

The fuel pressure during injection influences the spray pattern and the combustion delay. This effect is factored in by using the correction *P_fuel_corr*. The factor is used in the computation of the mass fraction burned during constant pressure and mass fraction burned during constant volume combustion. Increasing fuel injection pressure leads to higher value for the factor *(Figure 38)*.

The absence of cylinder pressure trace measurement makes it difficult to validate the modelled pressure. To avoid large deviations from actual cylinder pressure, a correction factor *P_em_corr*, dependent on the modelled exhaust pressure is used. The correction is a product with the in-cylinder pressure computed after TDC. The correction factor is used at each computation after TDC upto the exhaust *(Figure 39)*.

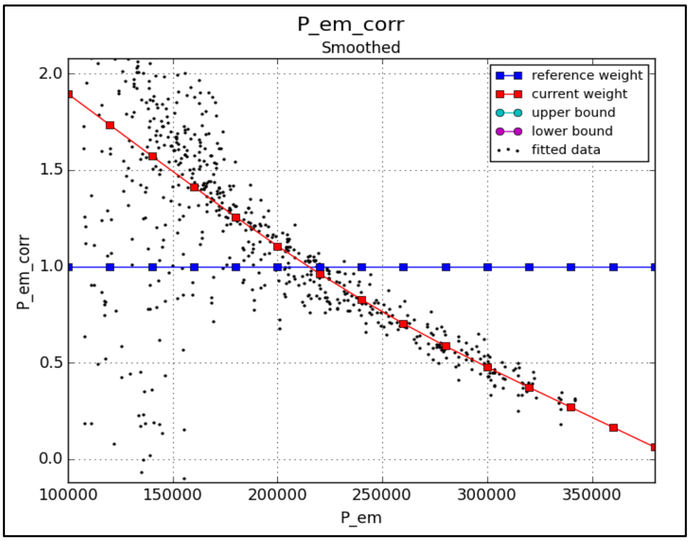

Figure 38 :- Correction of in-cylinder pressure, X- Exhaust manifold pressure.

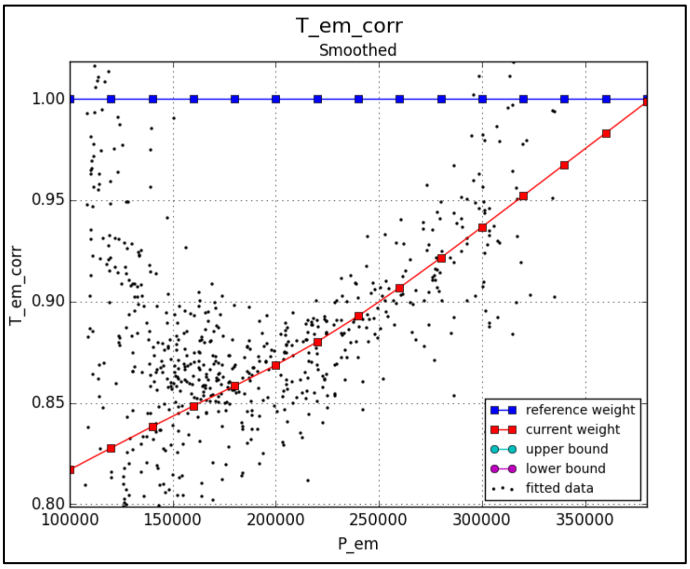

Figure 39 :- Correction of in-cylinder Temperature, X- Exhaust manifold pressure.

The introduction of a pressure correction based on exhaust gas temperature implies that a temperature adjustment would also influence the temperature levels. Therby a correction factor, *T_em_corr* is multiplied to the computed temperatures in the model *(Figure 40)*.

4.5 Assumptions in CAD resolved model

The resolution of computation for this model is every 10 crank angle degrees. This resolution is fixed for all operating conditions. The time scale for different speeds are different and lead to faster or slower changes in the system. But this model computes all operating conditions at the same resolution.

Valve opening and closing at different speeds leads to varying gas flows. This is not considered in the model. Rather, the valve events are assumed to be instantaneous and computations are made at these discrete crank angle degrees.

Only one main injection pulse is assumed to contribute to the combustion in the cylinder. Post and pilot injections are not considered for in cylinder combustion. The complete combustion of fuel injected in main injection is assumed.

The fuel is sprayed into the air charge in the cylinder. This results in charge cooling effect as the atomized fuel evaporates utilizing the heat from the air charge. This effect is also not taken into consideration.

In all operating points, the start of injection occurs a few crank angle degrees before or after the piston reaches TDC. Combustion is assumed in these cases to start at the instantaneous crank angle degree. Since no physical correlation is used for computing ignition delay, the phenomenon is compensated for by tuning the combustion duration itself.

Heat transfer in the port is computed by using one single control volume. This averaged computation leads to loss of some accuracy and can be improved by considering several other control volumes.

5. Results and Discussions

5.1 Dual Cycle Model Tuning

The dual cycle based model is developed by tuning several parameters in the model and by realizing the model using physical equations as discussed in previous sections. Two types of data set were used to tune the model. The focused tests are a combined set of data from a specific set of tests in the engine rig as discussed earlier. The second set of combined data is data recorded during part load tests. The steady state values of the modelled exhaust temperature are compared to the measured values in the dataset.

5.1.1 Focused Test combined

The datasets for four different engine tests are combined to form a single larger data base. The same is used to tune the Dual Cycle model. The modelled and the measured exhaust temperature is plotted for comparison and analysis *(Figure 41)*.

The scatter of the several data points makes it difficult to visually evaluate the accuracy of the model. Although it is clear that the model is unable to capture several localized linear temperature profiles for steady states in close proximity. This phenomenon can be attributed to the transient effects that were captured in the measured exhaust temperature at the test rig *(Figure 42)*.

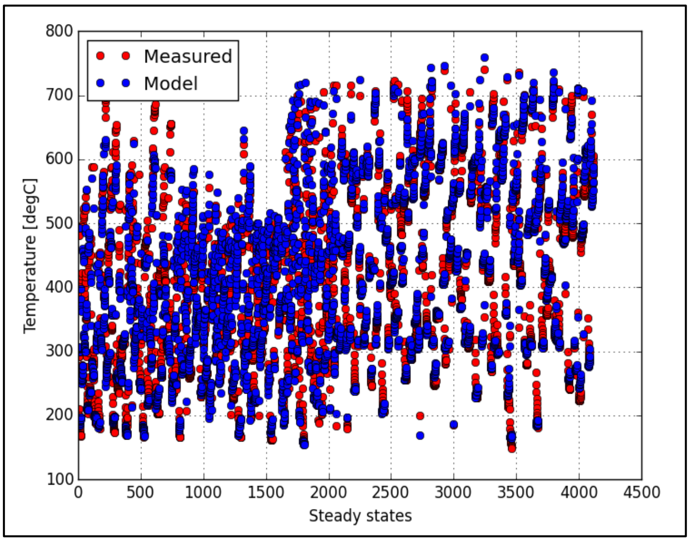

Figure 40 :- Exhaust gas temperature at end of exhaust port, Modelled and Measured

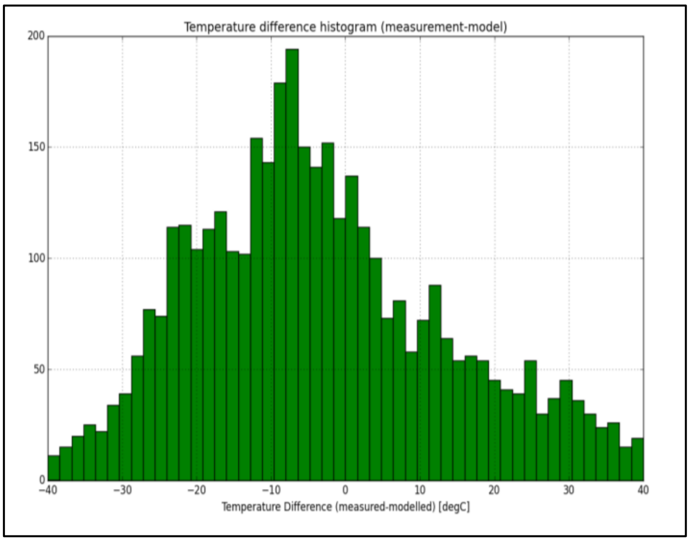

Figure 41 :- Histogram of temperature difference between measured and modelled Exhaust gas temperature

The histogram of error between the modelled and measured temperatures, gives a better visualization of the error distribution. The root mean squared error of the exhaust temperature is 27 degrees Celsius.

5.1.2 Part load combined

The engine test data for part load test of the engine are used to tune the model. This consists of a combination of three different part load tests. The exhaust temperature from these datasets is compared with the modelled value. The tuning parameters are of two types, one which is dependent on a varying parameter along the operating region of the engine. The other is an optimized constant which has the same value for all operating points *(Table 1)*.

Tuning parameters of the constant type are optimized for the entire dataset. The optimum values of these parameters are enlisted in the table below.

Table 1 :- Optimized constants for the dual cycle model, part load test data

Parameter	Tuned value	Unit	Parameter	Tuned value	Unit
Ac_w	0.0049	m^2	**C1**	68.32	--
Ag_w	0.0049	m^2			

The model is tuned to the dataset and the calibrated parameters are used to compute the final temperature of the exhaust. This exhaust temperature is compared to the measured value in the test rig at the end of the exhaust port in the engine *(Figure 43)*.

The model follows well the measured value at mid range temperatures. But the low temperature trends lose accuracy in the model *(Figure 44)*

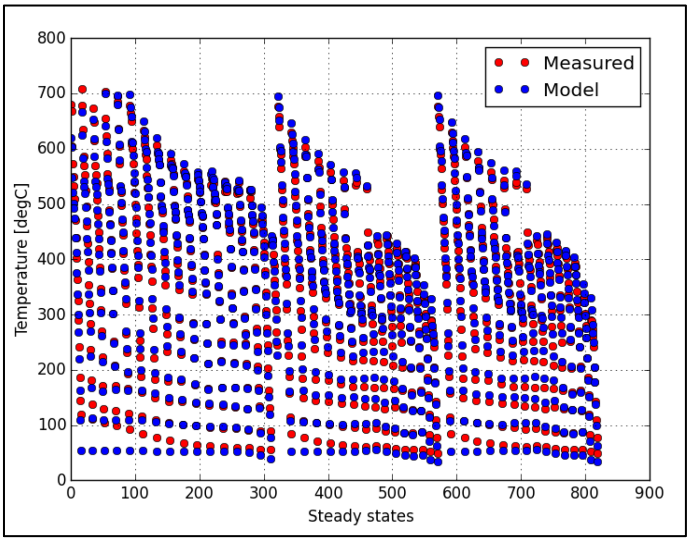

Figure 42 :- Exhaust gas temperature at end of exhaust port, Modelled and Measured

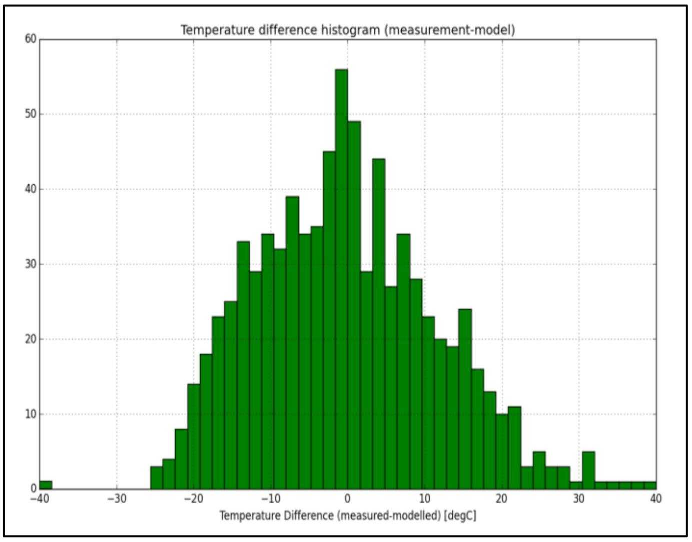

Figure 43 :- Histogram of temperature difference between measured and modelled Exhaust gas temperature

The histogram of errors between the modelled and the measured is plotted to understand the spread of the error across the test data. The root mean squared error of the exhaust temperature for this model is 9 degree Celsius. The maximum number of data points lie at the zero-error part of the histogram, indicating close following of the model with the measurement.

5.2 CAD Resolved Model Tuning

The CAD resolved model is developed by tuning several parameters in the model and by realizing the model using physical equations along with actual valve and injection events as discussed in previous sections. Two types of data set were used to tune the model. The focused tests are a combined set of data from a specific set of tests in the engine rig as discussed earlier. The second set of combined data is data recorded during part load tests. The trends of the tuned parameters are discussed and the modelled value of exhaust temperature are compared to the measured values in the dataset.

5.2.1 Focused Test combined

The datasets for four different engine tests are combined to form a single larger data base. The same is used to tune the CAD Resolved model. The measured and modeled values of exhaust temperature are plotted to understand the model accuracy *(Figure 45)*.

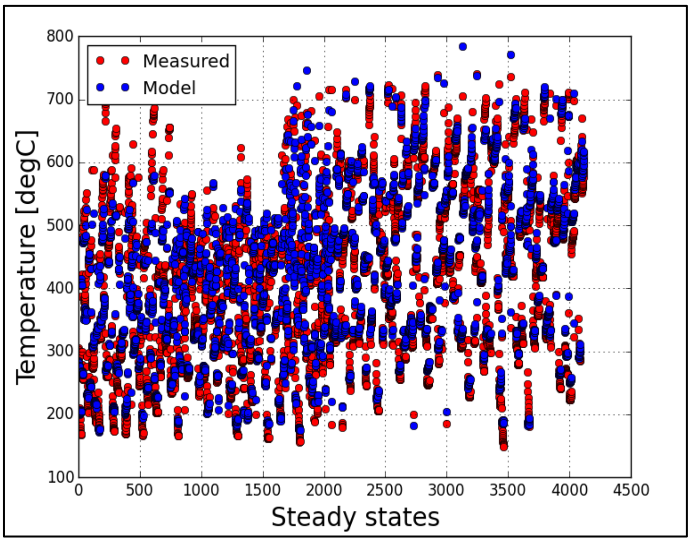

Figure 44 :- Exhaust gas temperature at end of exhaust port, Modelled and Measured

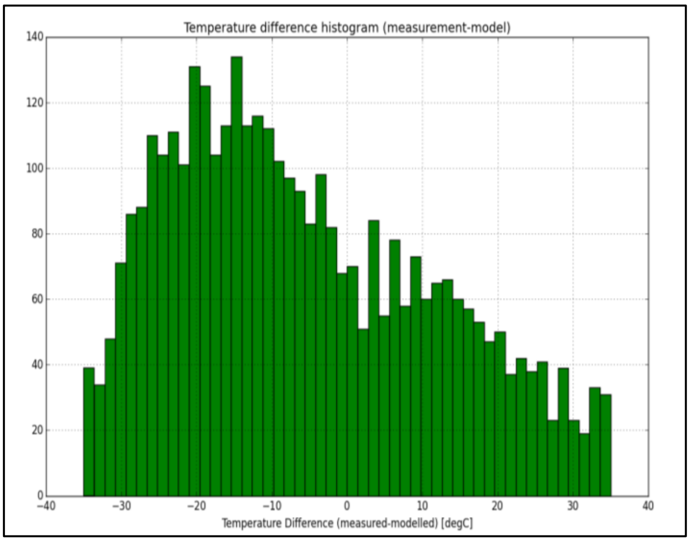

Figure 45 :- Histogram of temperature difference between measured and modelled Exhaust gas temperature

The scatter of the several data points make it difficult to visually evaluate the accuracy of the model. The model is unable to capture several localized linear temperature profiles for steady states in close proximity. This phenomenon might be as a result of transience effects that were captured in the measured exhaust temperature at the test rig *(Figure 46)*.

The histogram of error between the modelled and measured temperatures, gives a better visualization of the error distribution. The root mean squared error of the exhaust temperature is 26 degrees Celsius. The error in this case is shifted more towards the negative axis direction. This implies that the modeled temperature in most cases is higher than the measured values.

5.2.2 Part load combined

The engine test data for part load test of the engine are use d to tune the model. This consists of a combination of three different part load tests. The control signals from the data set are used in the model and the final temperature of the exhaust is compared with the modelled value. There are several other tuning parameters in the model which are tuned to achieve a desired level of model accuracy. Some of the constant tuned parameters are enlisted below in *(Table 2)*.

Table 2 :- Optimized constants for the CAD resolved model, part load test data

Parameter	Tuned value	Unit	Parameter	Tuned value	Unit
Ac_w	0.0049	m^2	**M1**	4.0378	--
Ag_w	0.0018	m^2	**M2**	1.604	--
C1	49.67	--			

The modeled temperature of the exhaust gas closely follows the measured values of exhaust gas temperature. This can be observed by plotting the measured against the modelled values *(Figure 47)*.

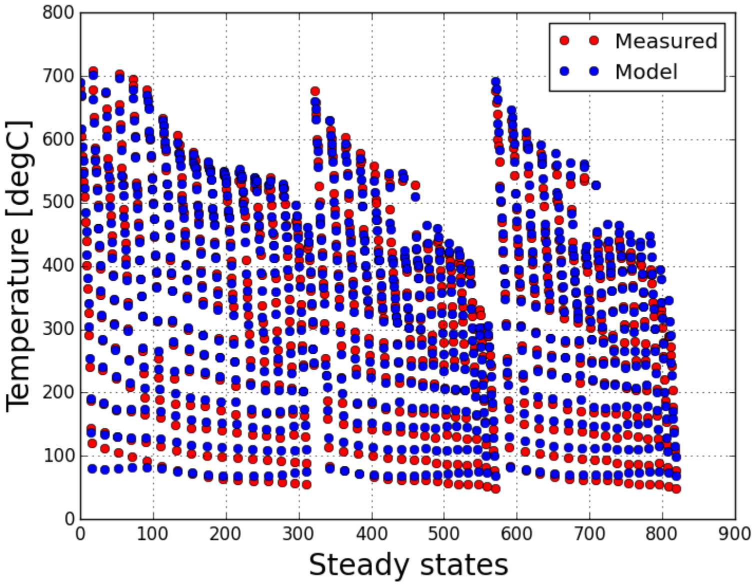

Figure 46 :- Exhaust gas temperature at end of exhaust port, Modelled and Measured

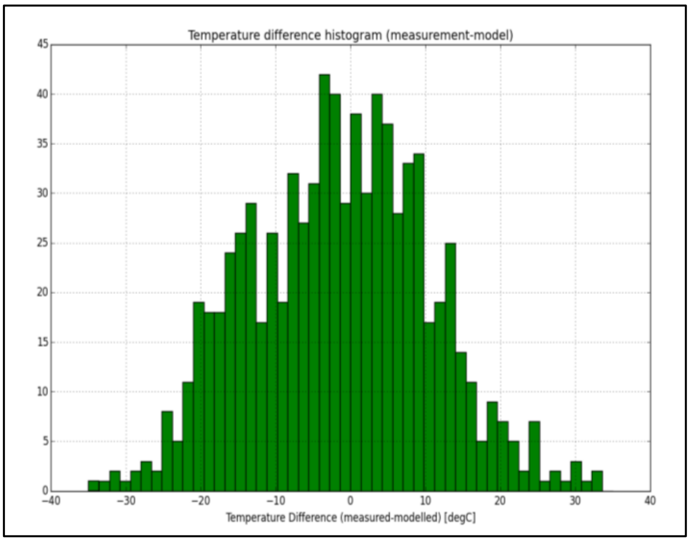

Figure 47 :- Histogram of temperature difference between measured and modelled Exhaust gas temperature

The accuracy is higher in the mid temperature ranges and is low in the low temperature range. Trends in the higher temperature range are also well captured by the model *(Figure 48)*.

The temperature difference between the modelled and the measured temperature is the error. The error is plotted as a histogram to understand the spread of the error. As in the above figure, most of the steady state point error lies within +/- 20 degrees Celsius. The root mean squared error is computed for this distribution and is found to be 13. The apparent bell curve shape of the distribution has its maximum close to zero.

6. Conclusion

The map based approach of modelling the engine out exhaust gas tends to be a black box model where correlation to physical phenomenon is difficult. The accuracy achieved in the physical models built using two different approaches, indicate a possibility of being able to switch to a physical model. The focused test data set do not yield desired results and the main reason is attributed to the transience in the measurement of the data itself, as discussed in the previous sections. The part load tests however are apparently devoid of this measurement transience as loads shift gradually. The CAD resolved model and the Dual cycle model are well tuned for these data sets and have achieved the desired level of accuracy. The Crank angle resolved model can achieve an RMS value of about 13 while the RMS in case of the Dual cycle model is 9 *(Figure 49)*.

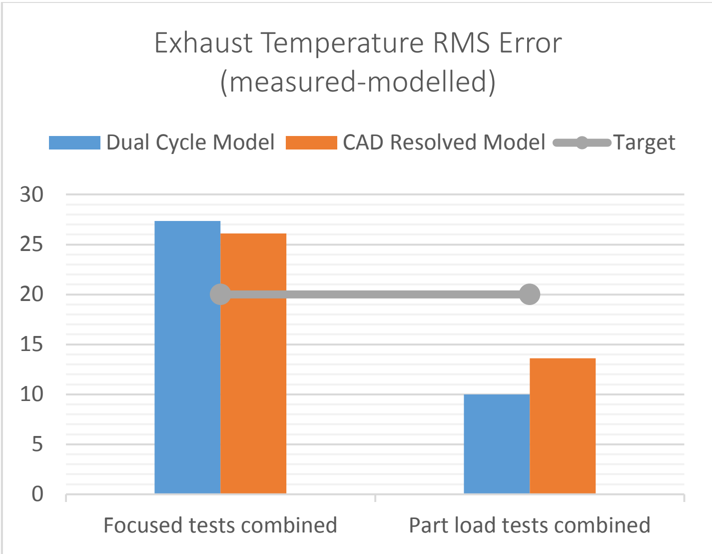

Figure 48 :- Exhaust gas temperature RMS error

A preferred choice among the two physical approaches, seems to be the dual cycle model. This model is not only simpler but also gives a better accuracy with respect to the available datasets. The crank angle degree model is more physically based as it has a higher resolution of computation and also heat release phenomenon is structured on the basis of typical Wiebe correlation. With the inclusion of the transient equations in the physical model, it would be possible to implement the model in the existing control system.

7. Future Scope

Data acquisition: cylinder head and cylinder liner temperature measurements can be used to further calibrate the model. This provides scope to be able to correspond to the actual wall temperature and will give a better estimation of the heat loss.

Transient model tuning and validation: The transient equations can be included in the current model to be able to have it running in the control system in real time.

Increase model complexity: drive modes & other effects can be included to capture other phenomenon or operating modes in the engine.

Analyse and validate with larger and more data sets: More datasets from test cell can make the model more robust and can improve the calibration of the model parameters resulting in improved accuracy of the model output.

Bibliography

[1] J. B. Heywood, Internal Combustion Engine Fundamentals, New York: McGraw-Hill, 2011.

[2] P. Skogtjran, "Modelling of the exhaust gas temperature for the diesel," MSc thesis in Vehicular Systems Linköping university, 2002.

[3] A. Verem and H. Kerai, "Physically Based Models for Predicting Exhaust Temperatures in SI Engines," M. Sc. Thesis, Department of Electrical Engineering, Linköping University, 2016.

[4] "Engineersedge," 2017. [Online]. Available: http://www.engineersedge.com/heat_transfer/convective_heat_transfer_coefficients__13378.htm (Available 2017 June)